

# **Unified Power Flow Controller (UPFC)**

## **Development of the mathematical framework and design of a transient model**

**Manish Thakur**

A thesis

submitted in partial fulfilment of the requirements

for the degree of Master of Science

The University of Manitoba

Department of Electrical and Computer Engineering

Winnipeg, Manitoba, Canada

February 2004

**THE UNIVERSITY OF MANITOBA**

**FACULTY OF GRADUATE STUDIES**

**\*\*\*\*\***

**COPYRIGHT PERMISSION**

**Unified Power Flow Controller (UPFC)  
Development of the Mathematical Framework and Design of a Transient Model**

**BY**

**Manish Thakur**

**A Thesis/Practicum submitted to the Faculty of Graduate Studies of The University of  
Manitoba in partial fulfillment of the requirement of the degree**

**Of**

**MASTER OF SCIENCE**

**Manish Thakur © 2004**

**Permission has been granted to the Library of the University of Manitoba to lend or sell copies of this thesis/practicum, to the National Library of Canada to microfilm this thesis and to lend or sell copies of the film, and to University Microfilms Inc. to publish an abstract of this thesis/practicum.**

**This reproduction or copy of this thesis has been made available by authority of the copyright owner solely for the purpose of private study and research, and may only be reproduced and copied as permitted by copyright laws or with express written authorization from the copyright owner.**

## **Abstract**

The Unified Power Flow Controller (UPFC) is one of the modern power electronics devices that can be used for the control of real and reactive power in a transmission line. The UPFC uses voltage sourced converter (VSC) technology to inject a series voltage with the sending end ac source to achieve its control objective with high speed, making it suitable for maintaining the voltage and mechanical stability of a network.

Using circuit theory, this thesis first develops the operating regimes of the UPFC and identifies how the injected voltage affects the flow of real and reactive power. Based on this analysis, various control schemes are designed and analyzed. It is possible to develop an open-loop control scheme, which works well in the steady state, but shows undesirable transients in the control of say, reactive power when the real power is changed. It is also not accurate if the system data on which it is based is approximate.

Another possibility is to use closed loop control, which overcomes the approximate nature of open loop control. It is shown that using known transmission line parameters, this closed loop controller can be made to have independent control of real and reactive control.

The thesis develops models for the above controllers and demonstrates their comparative performance using an electromagnetic transients simulation.

## **Acknowledgements**

The author expresses his gratitude to his advisor Prof. A.M Gole for his valuable support, encouragement and advice all throughout. Working under his guidance has been an enriching experience in more than one ways.

The author wishes to thank Dr. David Jacobson as co-advisor and Manitoba Hydro.

Special thanks to my Power Tower colleagues Chris, Phil and visiting Prof. I Paptic for their valuable technical discussion and support.

Finally, I am grateful to my wife, Ranju.

Manish Thakur

Winnipeg, Feb, 2004

# Table of Contents

---

## *LIST OF FIGURES III*

## *LIST OF SYMBOLS V*

<b>CHAPTER 1</b>	<b><i>INTRODUCTION</i></b>	
	Review of AC Power Transmission .....	1
	Focus of the Research Subject .....	3
	<i>Unified Power Flow Controller (UPFC)</i> .....	5
	<i>Research Tool: PSCAD/EMTDC</i> .....	5
	Overview of the Research Report .....	6
<b>CHAPTER 2</b>	<b><i>VOLTAGE SOURCED CONVERTER (VSC) TOPOLOGIES</i></b>	
	Basic Principles .....	8
	Voltage Sourced Converter Components .....	9
	<i>DC Voltage Source</i> .....	9
	<i>Power Converter</i> .....	10
	Voltage Sourced Converter Switching and Harmonic Components ..	12
	Voltage Sourced Converters Topologies .....	14
	<i>Static Synchronous Compensator (STATCOM)</i> .....	15
	<i>Static Synchronous Series Compensator (SSSC)</i> .....	17
	<i>Unified Power Flow Controller (UPFC)</i> .....	18
<b>CHAPTER 3</b>	<b><i>ANALYTICAL STUDIES OF TRADITIONAL POWER FLOW CONTROLLERS OF AN AC NETWORK</i></b>	
	Simple point to point Power flow within an AC transmission network	21

	Traditional transmission line compensation and power flow control within AC transmission network .....	24
	<i>Ideal MidPoint Shunt Compensator</i> .....	24
	<i>Series Compensation</i> .....	27
	<i>Phase Angle Control (PAR)</i> .....	30
	Summary .....	32
<b>CHAPTER 4</b>	<b><i>MATHEMATICAL MODEL OF UPFC.</i></b>	
	Power flow of a transmission line with UPFC .....	33
	Independent Control of Real and Reactive Power Flow .....	38
	Control methods of UPFC .....	40
	<i>Control Methods of Shunt Converter</i> .....	41
	<i>Control Methods of Series Converter</i> .....	47
	<i>Decoupled Control Method based on d-q axis</i> .....	51
	Overall Control System for the Complete UPFC .....	54
<b>CHAPTER 5</b>	<b><i>MODELING OF UPFC USING PASCAD/EMTDC.</i></b>	
	Introduction .....	55
	Modeling of a Series Converter .....	56
	<i>PWM based d-q controller for the Series Converter of UPFC</i> .....	61
	<i>Decoupled d-q axis controller for the Series Converter of UPFC</i> .....	64
	Modeling of the full UPFC .....	71
	Improvement for Control Implementation in Actual Network .....	78
<b>CHAPTER 6</b>	<b><i>CONCLUSIONS AND RECOMMENDATIONS</i></b>	
	Conclusions .....	81
	Further Recommendations .....	83
<b>APPENDIX A</b>	<b><i>SINUSOIDAL PULSE WIDTH MODULATION</i></b>	
<b>APPENDIX B</b>	<b><i>D-Q TRANSFORMATION OF THREE PHASE INSTANTANEOUS QUANTITIES.</i></b>	
	Introduction .....	87
	<b><i>REFERENCES</i></b>	
	References .....	91

## List of Figures

---

Manitoba-Ontario interconnection network .....	3
Voltage Sourced Converter Block Diagram .....	9
Two Level Six Pulse Voltage Converter .....	11
Three Level Bridge Voltage Converter .....	12
Converter Arrangement 6-Pulse *4 Converters = 24-Pulse Operation [12]. .....	14
Block Diagram of a Static Synchronous Compensator (STATCOM) .....	15
STATCOM Equivalent for Steady State .....	16
Block Diagram of a SSSC .....	17
VSC Based Unified Power Flow Controller (UPFC). .....	19
Simple AC Transmission Network .....	21
Transmitted $P_o(d)$ and $Q_o(d)$ Versus Phase Angle .....	23
Transmitted $Q_o(d)$ Versus $P_o(d)$ for $d$ (i.e. $0 \leq d < \pi/2$ ) .....	23
AC Transmission Network with MidPoint Shunt Compensator .....	25
Voltages and Currents Phasors of Shunt Compensator .....	25
Real & Reactive Power Versus Power Angle ( $d$ ) .....	26
AC Transmission Network with Series Compensation .....	28
Current and Voltage Phasors for Series Compensation .....	28
Real and Reactive Power Versus Phase Angle $d$ .....	29
AC Transmission Network with PAR .....	30
Current and Voltage Phasors of PAR .....	31
Real Power Versus Phase Angle ( $d$ ) .....	32
AC Transmission Network with UPFC .....	34
Range of Transmittable Power Versus Phase Angle ( $d$ ) of a UPFC .....	36
Range of Transmittable Real Power ( $P$ ) Versus Angle ( $d$ ) of a UPFC .....	37
Range of Transmittable Reactive Power ( $Q$ ) Versus Angle ( $d$ ) of a UPFC .....	37
Control Region of Attainable Real Power and Reactive Power with a UPFC for $d=0^\circ$ & $d=30^\circ$ .....	39
Control Region of Attainable Real Power and Reactive Power with UPFC for $d=60^\circ$ & $d=90^\circ$ .....	40

---

Basic Principal of Shunt Converter Operation .....	41
Simple Control System for Shunt Converter .....	42
Control Blocks for PWM Shunt Converter .....	44
Control Circuit for PWM STATCOM with steady state de-coupling loops .....	46
Open-Loop Control of a Series Converter .....	48
Equivalent Representation of Rectangular Coordinates .....	48
Slow Feedback Loop with Main Open-Loop Control .....	49
Closed Loop Partially Decoupled Control .....	50
Decoupled d-q Control loops of a Converter Connected to the System. ....	53
Modeling of Series Branch of UPFC .....	57
An Open Loop d-q Component Controller of the Series Branch of UPFC .....	59
Open Loop d-q Component Control method of a Series Converter .....	60
PWM based Series Converter .....	61
Firing Pulses of PWM for Series Converter .....	62
Phase Locked Loop of Series Converter .....	62
PWM based d-q Component control method of a Series Converter. ....	63
Simplified Equivalent AC transmission Network of a Series Connected Voltage Source Converter. ....	65
d-q Vector Transformation of Instantaneous Three Phase Quantities. ....	67
Decoupled d-q Controller of the Series Converter .....	68
Performance of decoupled d-q Controller. ....	70
Decoupled d-q Controller Based UPFC .....	72
Independent control of real and reactive power by UPFC .....	73
Series Converter's d-q axis Output Voltages $V_d$ and $V_q$ . ....	74
Capacitor Voltage of UPFC .....	75
Decoupled d-q Controller of the Shunt part of UPFC .....	76
Response of the shunt part of UPFC .....	77
Modified decoupled d-q control method. ....	79
Modified Decoupled d-q control of a Series Converter .....	80
Simple Voltage Sourced Inverter .....	84
Principal of Pulse Width Modulation .....	86
Vector Representation of Instantaneous Three Phase Variables. ....	88

## List of Symbols

---

**Table A.1 Operators**

*	Complex conjugate operator
$j$	Complex operator
$J$	Jacobian
$d/dt$	First order derivative

**Table A.2 Parameters**

$V_R$	Magnitude of voltage at receiving end of line $i$
$V_S$	Magnitude of voltage at sending end of line $i$
$V_r$	Magnitude of voltage at receiving end of line $i$
$V_s$	Magnitude of voltage at sending end of line $i$
$\angle\delta$	Phase Angle between the sending and receiving end
$X^{\text{mer}}$	Transformer
$P$	Real power flow of the transmission line
$Q$	Reactive power flow of the transmission line
$f$	System Frequency
$X$	Transmission Line Impedance (loss less)
$R$	Transmission Line Resistance
$P_o$	Uncompensated Real power flow of the transmission line
$Q_o$	Uncompensated Reactive power flow of the transmission line

**Table A.2 Parameters**

$P_c$	Compensated Real power flow of the transmission line
$Q_c$	Compensated Reactive power flow of the transmission line
$X_c$	Capacitive compensation
$s$	Phase Angle of the phase shifter
$\Delta V$	Magnitude of the injected voltage in series with the transmission line
$f$	Phase Angle of the injected voltage in series with the transmission line
$V_T$	STATCOM's ac side system voltage
$E_{a1}$	STATCOM's fundamental component of the switched voltage
$I_a$	A phase line current
$I_b$	B phase line current
$I_c$	C phase line current
$V_a$	A phase line voltage
$V_b$	B phase line voltage
$V_c$	C phase line voltage
$k_p$	Proportional gain
$k_i$	Integration constant
$dq0$	d-q converter block
$a$	Firing angle
$\theta_q$	Phase locked loop angle
$V_m(t)$	Reference voltage waveform for SPWM
$\text{Im}(V_m)$	Imaginary part of Reference voltage waveform
$\text{Re}(V_m)$	Real part of Reference voltage waveform
PI	Probational Integrator Controller
$P(t)$	Instantaneous Real Power
$Q(t)$	Instantaneous Reactive Power
$P^*$	Ordered real power flow
$Q^*$	Ordered reactive power flow
$i_d$ , or $I_d$	D axis current
$i_q$ , or $I_q$	Q axis current
$V_d$ , or $e_d$	D axis injected voltage
$V_q$ , or $e_q$	Q axis injected voltage
$D_{va}, D_{vb}, D_{vc}$	Sinusoidal Injected Voltages
$P_s$	Sending end Real Power
$Q_s$	Sending end Reactive Power
$P_{\text{shunt}}$ , or $P_p$	Real power of Shunt part
$Q_{\text{shunt}}$ , or $Q_q$	Reactive power of Shunt part

**Table A.2 Parameters**

---

$I_{pd}$	D axis current of shunt part
$I_{pq}$	Q axis current of shunt part
$V_{sd}$	D axis voltage of shunt part
$V_{sq}$	Q axis voltage of shunt part
$V_{dc}$	Capacitor Voltage
PSCAD/ EMTDC	Electromagnetic/Power System Simulation Software
PLL	Phase Locked Loop
VSC	Voltage Sourced Converter
GTO	Gate Turn Off Transistor
IGBT	Insulated Gate Bipolar Transistor
PLL	Phase Locked Loop
VSC	Voltage Sourced Converter
GTO	Gate Turn Off Transistor
IGBT	Insulated Gate Bipolar Transistor
SMES	Superconductive Magnetic Energy Storage
PWM	Pulse Width Modulation
PST	Phase Shift Transformer
SPWM	Sinusoidal Pulse Width Modulation
SSSC	Static Synchronous Series Compensator
STATCOM	Static Synchronous Compensator
SVC	Static Var Compensator
TCR	Thyristor Controlled Reactor
TSC	Thyristor Switched Capacitor
UPFC	Unified Power Flow Controller
IPFC	Interline Power Flow Controller

# CHAPTER 1 Introduction

---

## 1.1 Review of AC Power Transmission

Since the development of the transformer and AC transmission by L.Gaulard and J.D. Gibbs, electrical utility industries have opted AC over DC electric circuit for long distance power transmission. However, AC transmission involves both the real and reactive circuit parameters and variables which jointly determine the transmittable real power ( $P$ ) and overall transmission losses. The AC transmitted power for a given transmission line is defined by the transmission line impedance ( $X$ ), the magnitude of sending end ( $V_s$ ) and receiving end ( $V_r$ ) voltages, and the phase angle( $\delta$ ) between the end voltages. The basic operating requirements of an AC power system are that the synchronous generators must remain in synchronism and the voltages must be kept close to their rated values. In other words, the operating voltages are more or less fixed. Thus the steady-state power transmission capability of AC transmission line can be increased by providing reactive power ( $Q$ ) compensation (by changing  $X$ ).

Traditionally, the reactive power compensation [1], [2] and phase angle control [3] have been applied by fixed and mechanical switched circuit elements (capacitors, reactors and tap changing transformer) to improve the steady-state power transmission capability.

Due to the fact that the switching devices are mechanical and there is little high-speed control, the recovery from dynamic disturbance was accomplished by generous stability margins at the price of relatively poor system utilization.

In the late 1980's, due to the result of environment legislation, construction cost increase, and deregulation policies, there was a need to review traditional power transmit theory and practice, to create new concepts to utilize existing transmission system assets to the maximum extent possible. At the same time, the development of semiconductor technology, which made high voltage DC transmission possible, generated the curiosity to use power electronics to solve the outstanding problems of AC transmission.

Thus, it is in 1986 when the Electric Power Research Institute (EPRI) proposed the concept of "Flexible AC transmission system" (FACTS) [3] to solve the emerging system problems due to restriction on transmission line construction, and to facilitate the growing power demand among utilities. Later, the Institute of Electrical and Electronics Engineers (IEEE) and International Council of Large Electrical Systems (CIGRE) backed up the proposal which finally made FACTS a viable technology. The IEEE definition of FACTS is: "Alternating current transmission systems incorporating power electronics-based and other static controllers to enhance controllability and power transfer capability of AC transmission".

The development of FACTS devices has followed two distinctly different technical

approaches to target AC transmission problems.

- Thyristor Controlled FACTS Devices: TCR (Thyristor Controlled Reactors), TSCS(Thyristor Switched Capacitors) and Thyristor Controller Phase-shifter[2],[4].
- Voltage Source Converter based FACTS Devices: STATCOM (Static Compensator), SSSC (Static Synchronous Series Converter) [6],[7], UPFC (Unified Power Flow Controller) [5],[16]and IPFC (Interline Power Flow Controller)[8].

## 1.2 Focus of the Research Subject

In the absence of any mitigating devices such as a phase shifter transformer (PST), adjustment of the voltage magnitudes ( $V_s$ ,  $V_r$ ) of, or phase angle ( $\delta$ ) between the Manitoba-Ontario interconnection network to push more steady-state power into Ontario could inadvertently lead to power back to Manitoba through the Ontario-USA network. This circulating current, which is also referred to loop power flow, contributes system losses and may overload facilities of the other utilities. Thus steady-state power transmission may also be limited by so-called “loop power flows” shown in the Fig 1.1.

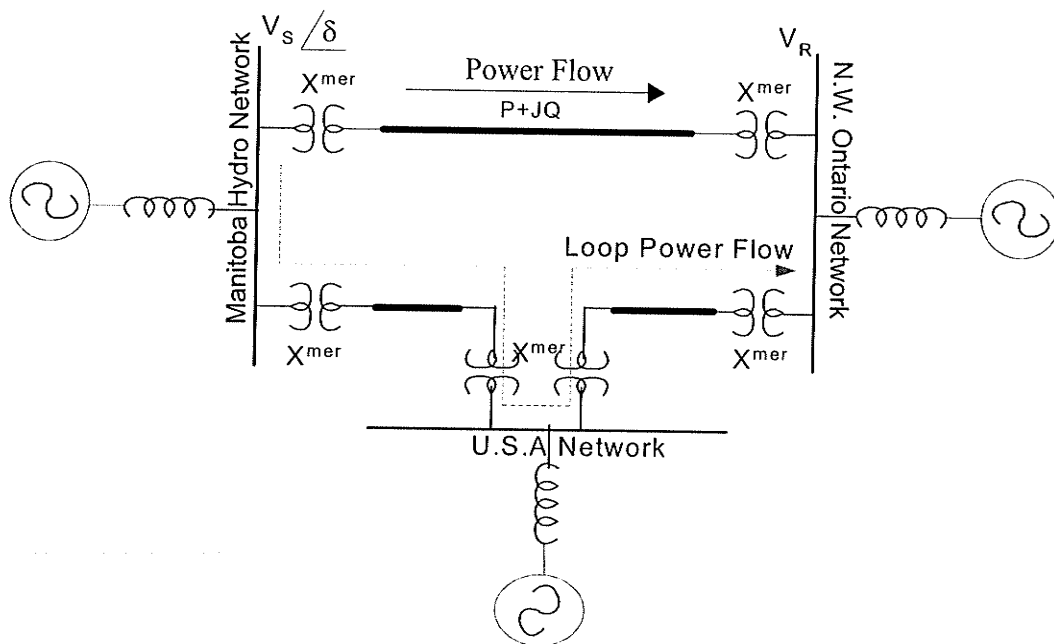


Fig. 1.1 Manitoba-Ontario interconnection network

To solve the above mentioned loop power flows, mechanical the PST [4] using on-load tap changers with quadrature voltage injection, was introduced in the 1930's to solve the "loop power flow" problem and to increase the utilization of AC transmission lines. The on-load tap changer with in-phase voltage injection controls reactive power via voltage magnitude adjustment and with quadrature voltage injection controls real power via phase magnitude adjustment. Their combined effect makes possible the control of both the real and reactive power flows. As a result the PST has been used to redirect current flows and alleviate inherent loop power flows in interconnected systems. The mathematical model of PST is described in chapter 3.

The conventional PST has the following disadvantages:

- (i) Slow response due to inherent inertia of the mechanical switches,.
- (ii) Limited life-time and frequent maintenance requirement of mechanical switches.

The first technical drawback limits the applications of conventional PST only to steady-state power flow and voltage regulation. The latter drawback can be partially overcome by using fast acting mechanical switches in addition to the slower mechanical ones.

Recently the emergence of FACTS devices such as the UPFC with promises of providing independent control of the real and reactive power of the transmission line inspired the thesis; as the UPFC may be a viable alternative to the traditional PST.

Hence the focus of the research is to study and the analyze the various control methods of UPFC in a given AC transmission network.

### **1.2.1 Unified Power Flow Controller (UPFC)**

The UPFC [5] is a member of the FACTS family of compensators and power flow controllers, which utilizes the synchronous voltage source (SVS) [6], [7] concept for providing a unique capability for transmission system control. Within a framework of traditional power transmission concepts, the UPFC is able to control, simultaneously or selectively, all the parameters affecting power flow in the AC transmission line (i.e. voltage, impedance, and phase angle) and through rapid control action, mitigate dynamic disturbance. At the same time, it can provide the unique functional capability of independently controlling both the real and reactive power flow in the AC transmission line.

### **1.2.2 Research Tool: PSCAD/EMTDC**

PSCAD is the most popular electromagnetic simulation program used in the electric utilities, electrical equipment manufacturers and research and academic institutions to perform modeling of multi-phase electrical power systems, power electronic devices and control networks. PSCAD, a time domain program, is mainly dedicated to study transients in electric power systems.

A built in library of advanced components ranging from simple passive elements and control functions, to sophisticated power electronic controls and complex power system models (electric machines, transmission lines and cables) allows a user to precisely design and simulate all types of power systems including power electronics devices. This tool is used for developing the UPFC model for transient studies.

### 1.3 Overview of the Research Report

**Chapter 2** gives a general introduction to power electronics devices applications based on VSC topologies such as STATCOM, SSSC and UPFC. The operating principles of VSC devices are discussed.

**Chapter 3** describes an analytical study of traditional AC transmission line compensations and power flow control methods. In this section, basic approaches such as ideal shunt-connected var compensation, series compensation, and phase angle regulation to increase the transmittable power over AC transmission lines are discussed and compared.

The understanding of these basic approaches provides the foundation for power electronics-based reactive power compensation and control techniques capable of increasing steady-state power flow.

**Chapter 4** derives a mathematical model of UPFC for a given transmission line to understand its basic operating principles. This model is used to investigate the capability of UPFC to control independently steady-state real and reactive power flows in the transmission line. The mathematical model is also used to design various control schemes such as Open Loop, Coupled and Decoupled control blocks of UPFC, and then compare control schemes performance in offering independent control of real and reactive power. The later part of the research will discuss overall control system of a UPFC model.

**Chapter 5** discusses the development of a UPFC model on PSCAD/EMTDC simulation software for transient studies. The modeling of the UPFC begins from developing the

---

model of a Series Converter, which is the principal operational converter, and then apply learnt control blocks such as open loop and decoupled d-q on Series Converter. UPFC simulation results of various applied control blocks will be compared with the derived mathematical model for an independent control of the P and Q power flows of the system within the specified range defined by the maximum limit of series injected voltage.

**Chapter 6** provides a conclusion by confirming the independent control of real and reactive power flow of the transmission line of UPFC and also provides future possibilities of applying UPFC in various applications of AC transmission network.

## CHAPTER 2 Voltage Sourced Converter (VSC) Topologies

---

The Voltage Sourced Converter (VSC) is a fundamental building block of a large class of FACTS devices such as UPFC and IPFC. This chapter will first discuss the building block of a voltage source converter, which is then extended to more complex topologies to accomplish a UPFC block.

### 2.1 Basic Principles

VSC can produce three alternating voltages from a DC source by means of high speed solid state switches. The solid state switches allow one to obtain a fast and fully controllable amplitude and phase angle in the alternating voltage. From a fundamental frequency viewpoint, this behaves in a manner similar to a synchronous AC machine connected to an AC network. Like the AC machine, the VSC presents itself as a voltage behind an inductance. Some of the desirable characteristics of the rotating machine are: high capacitive output current at low system voltage levels and an essentially inductive source impedance that cannot cause harmonic resonance with the network. On the other hand some draw-

backs are slow response, potential for rotational instability and high maintenance. These disadvantages are considerably reduced with the solid state VSC.

## 2.2 Voltage Sourced Converter Components

The main components of a VSC are depicted in the block diagram shown in the Fig 2.1. The DC voltage block supplies voltage to a Power Converter which by operation of its solid state switches (Gate Turn Off (GTO) or Insulated Gate Bipolar Transistor (IGBT)) generates an AC waveform in the transformer side. Through the control of the magnitude and phase angle of this AC waveform the real and reactive power entering the AC network can be precisely controlled.

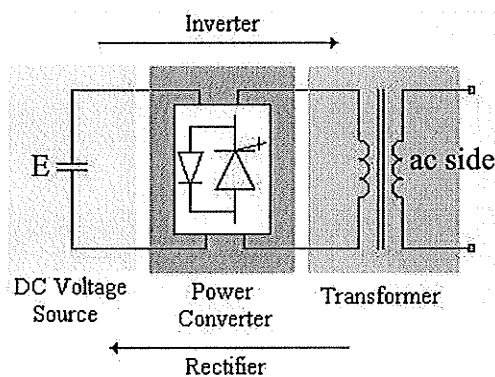


**Fig. 2. 1** Voltage Sourced Converter Block Diagram

### 2.1.1 DC Voltage Source

The DC voltage source can be one of several alternatives. In the simplest form, it is simply a charged capacitor. If energy exchange is important, a battery or even another converter can be used. Other arrangements include a voltage source generated by connecting a

power conditioner to a superconducting inductive coil (Superconducting Magnetic Energy Storage “SMES”).

### 2.1.2 Power Converter

The VSC described above can be configured in a “bridge” arrangement. The simplest bridge types are two-level bridges and three level bridges. In the two level bridge as shown by Fig 2.2, the AC voltage is generated by alternately connecting the output terminal to one of two DC levels ( $+V_{dc}/2$  and  $-V_{dc}/2$ ). This is accomplished through the appropriate turn on and turn off of the switches, each one of which consists of a controllable element (GTO or IGBT) in anti parallel with a diode. The DC voltage is supplied by a capacitor, battery or another power converter and it is ideally constant. If the net power taken from the source is zero, a capacitor may be used in place of the DC source. The capacitor should be small because of economic reasons. On the other hand the use of a small capacitor may generate a larger ripple in the DC-Link voltage during steady-state operation and even greater impact on the DC voltage as a consequence of system disturbances. The choice of the capacitor is a compromise.

In the three level bridge topology as shown by Fig 2.3, the DC capacitor is divided into two equal sections with equal voltage across each section. The semiconductor valves connect each phase to three different voltage levels ( $+V_{dc}$ , Zero (Midpoint) and  $-V_{dc}$ ). For this arrangement six diodes are required as in Fig 2.3. In this arrangement, the zero voltage is obtained if the two switches in the middle are turned on.  $+V_{dc}$  is applied to the output if the two upper switches are turned on while  $-V_{dc}$  is obtained if the lower two switches are fired.

One of the advantages of this technique is the possibility to set the pulse width (see  $\alpha$  Fig 2.3) in such a way that a selected harmonic can be eliminated. Converters with more than three levels are not a common option in the market due to their complexity.

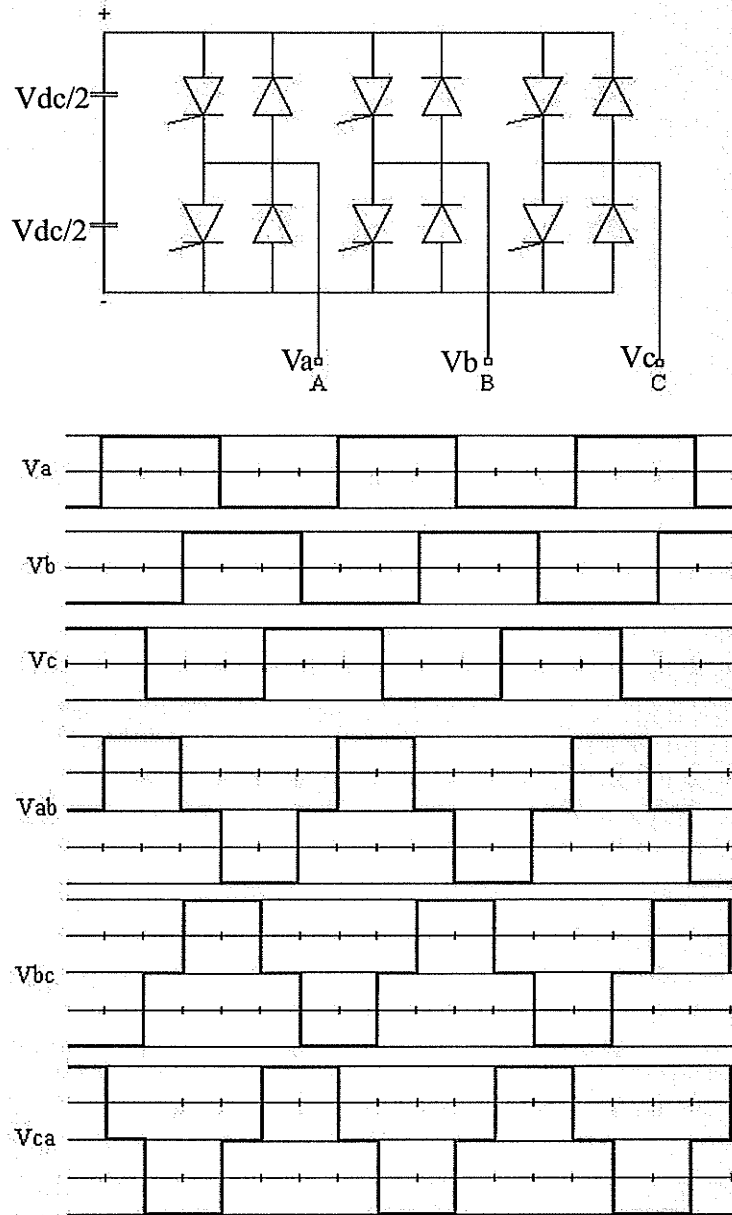


**Fig. 2. 2** Two Level Six Pulse Voltage Converter

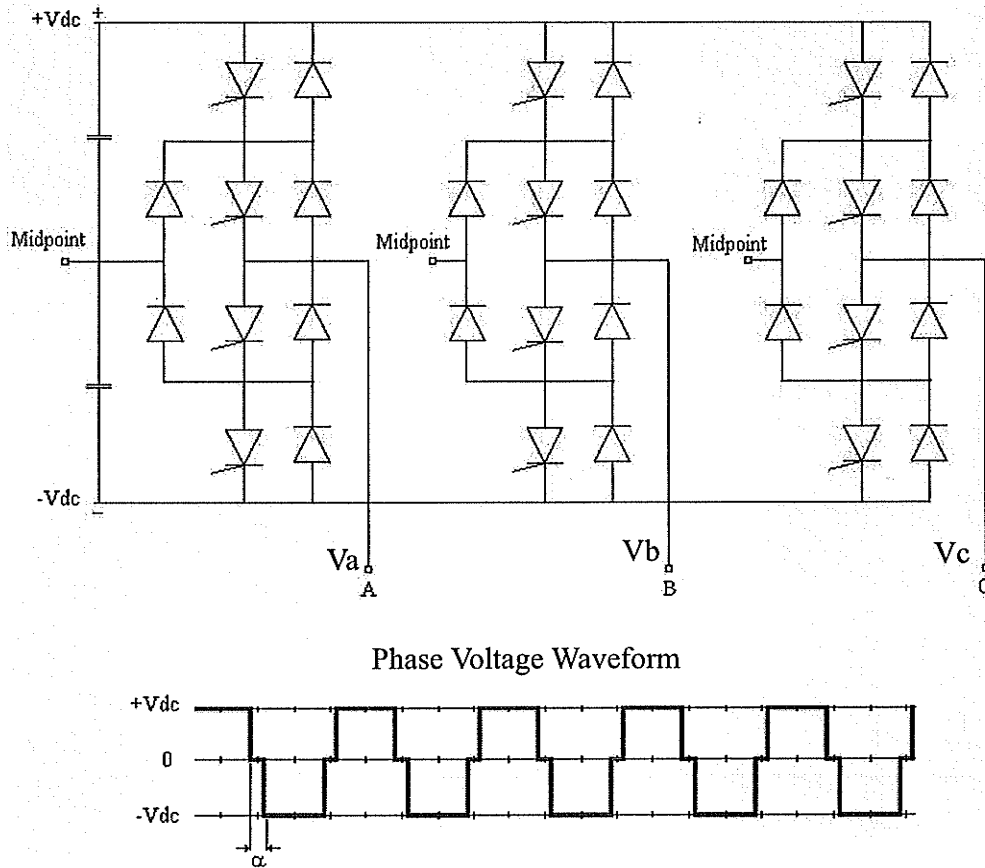


**Fig. 2. 3** Three Level Bridge Voltage Converter

## 2.2 Voltage Sourced Converter Switching and Harmonic Components

In high power applications, the switching frequency can be classified as follows. Fundamental frequency switching (60 Hz) is considered as low frequency. Medium switching frequency can be defined between 5 to 9 times fundamental frequency (300 Hz to 540 Hz). High frequency is above 15 times the fundamental frequency ( $> 900$  Hz) [9].

An important task of the switching technique is the reduction of harmonic content generated by the converter. Many techniques have been developed throughout the years, from

the basic six-pulse, to Pulse Width Modulation (PWM), and Optimal Pulse Width Modulation (OPWM) where the switching angles are calculated in order to avoid certain harmonics components [10]. Although Pulse Width Modulation (PWM) creates high switching losses in the power semiconductors, the continuing improvements in semiconductor technology still makes this technology potentially attractive.

If the switches are operated at fundamental frequency, with  $120^\circ$  phase shifting, to connect the DC supply sequentially to the outputs, then a balanced set of three square waves ( $V_a$ ,  $V_b$  and  $V_c$ ) is obtained as shown in Fig 2.2. In a three phase system with delta connected converters (isolated neutral), the triplen order harmonics 3rd, 9th, 15th, etc, will be only of zero sequence and therefore they will not flow in the line currents, unless the supply voltage or the converter become unbalanced.

The output DC voltage waveform of the six-pulse converter normally contains harmonic components of frequency  $(6k \pm 1) \cdot f$  where  $f$  is fundamental frequency and the DC side current has harmonic components  $6k \cdot f$  and  $k = 1, 2, 3, \dots$ . The large amount of harmonic content in the output voltage makes it unsuitable device for high power applications. Nevertheless using the principle of harmonic neutralization using  $n$  basic six-pulse converters operated with certain phase shifting between them allows us to obtain an overall  $P = 6n$  multi pulse arrangement shown in Fig 2.4. The harmonic frequencies present in this  $P$ -pulse arrangement are  $(Pk \pm 1) \cdot f$  for output voltage and  $Pk \cdot f$  for input current [10]. Multi pulse (harmonic neutralized) converters can be implemented by a variety of circuit arrangements using different magnetic devices [11], [12], [13].

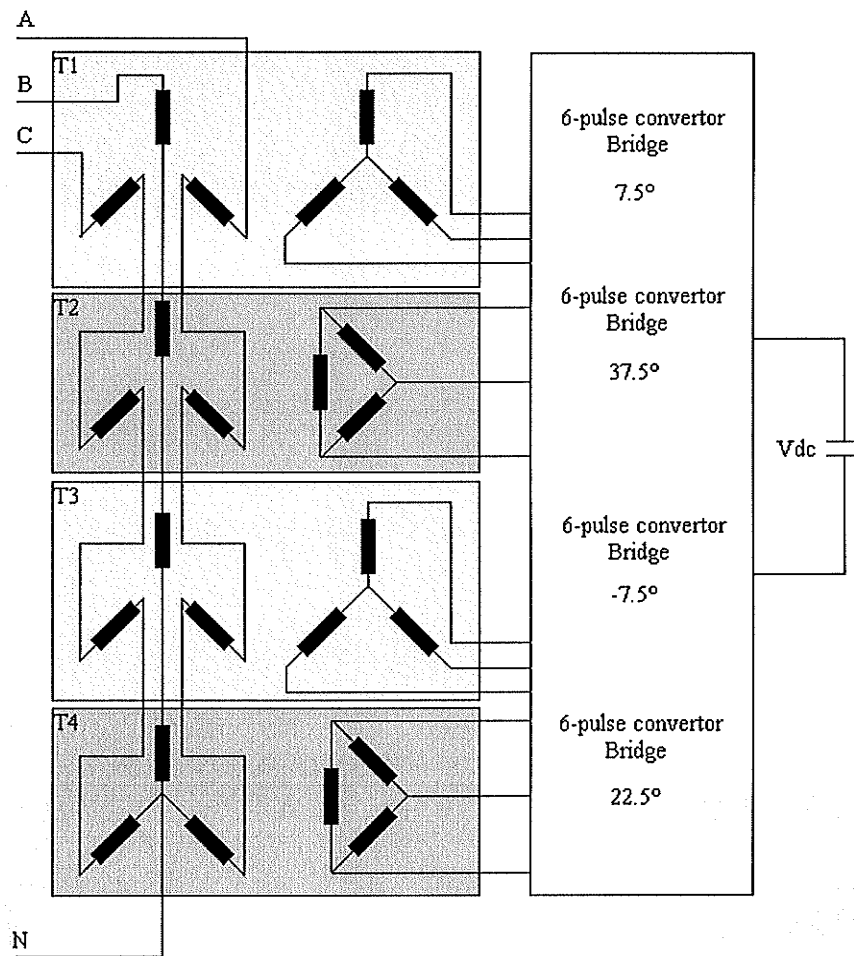


Fig. 2. 4 Converter Arrangement 6-Pulse \*4 Converters = 24-Pulse Operation [12].

### 2.3 Voltage Sourced Converters Topologies

The VSC is the genesis of many controllers, nevertheless the main topologies are STATCOM and SSSC).

### 2.3.1 Static Synchronous Compensator (STATCOM)

The STATCOM [10], [14] is a VSC that converts a DC voltage into a three-phase output voltage at fundamental frequency, a coupling transformer and a DC source (capacitor, SMES, Battery Energy Storage System (BESS), etc). The steady state operation is similar to that of a rotating synchronous compensator but without inertia, so STATCOM's response is basically instantaneous and does not significantly alter the existing system impedance. It is an advance over SVC.

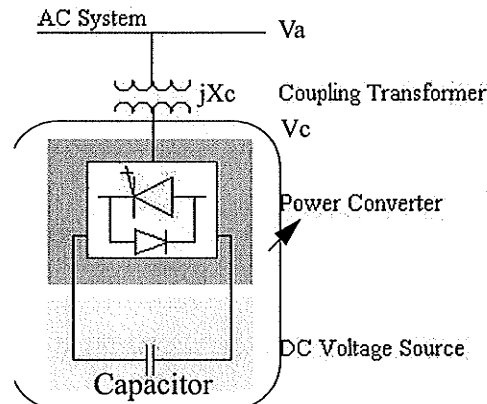


**Fig. 2.5** Block Diagram of a Static Synchronous Compensator (STATCOM)

The arrangement in Fig 2.5 shows a typical STATCOM, in which the steady state power exchange between the device and the AC system is mainly reactive. The power exchange is controlled by regulating the amplitude of the STATCOM output voltage ( $V_c$ ). If the per-unit amplitude of STATCOM output voltage ( $V_c$ ) is larger than the per-unit amplitude of the AC system ( $V_a$ ), the device generates reactive power (capacitive). On the other hand if the STATCOM output voltage is lower than that of the AC system, the device will absorb

reactive power (inductive). The capacitive and inductive reactive power compensation modes can be easily understood from the phasor diagram shown in Fig 2.6.

Note if both AC system and STATCOM have the same voltage, there is no power exchange. The current from the STATCOM is 90° shifted with respect to the ac system voltage ( $V_a$ ), and it can be leading (generates reactive power) or lagging (absorbs reactive power) [15].

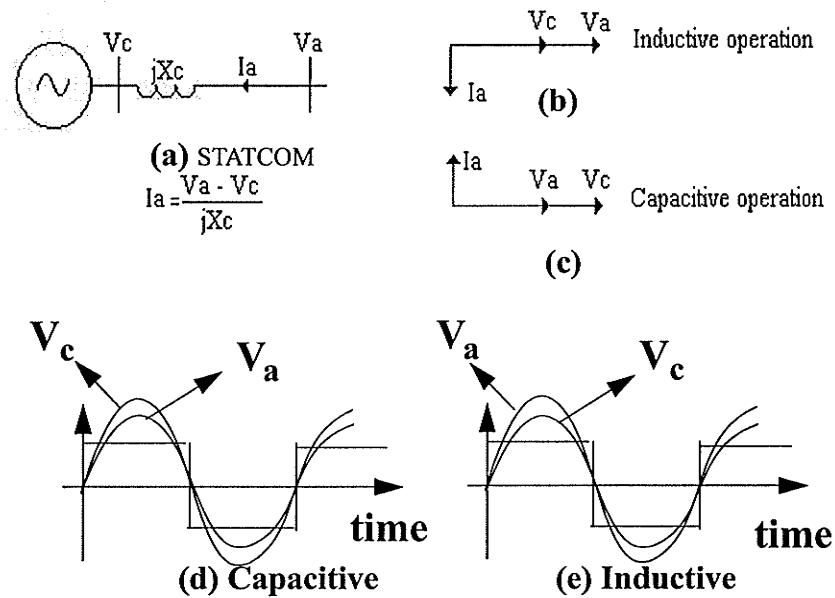


Fig. 2. 6 STATCOM Equivalent for Steady State

In above case a capacitor is used to supply DC voltage to the converter. However the converter keeps the capacitor charged to the levels set. In the steady operation the phase angle between  $V_a$  and  $V_c$  is kept at 0°. By marginally shifting it from 0°, real power can be made

to flow into or out of the VSC, thereby charging or discharging the DC capacitor. This mechanism is used to keep the capacitor voltage constant if needed. In fact, in the steady state, the output voltage of the inverter slightly lags the AC system voltage, so that a small amount of real power from the system flows into the VSC to compensate for internal losses and thus, keeping the capacitor voltage constant.

### 2.3.7 Static Synchronous Series Compensator (SSSC)

When VSC is connected through a coupling transformer in series with the power transmission line, this arrangement results into a new device called SSSC [6]. The SSSC is shown in Fig 2.7

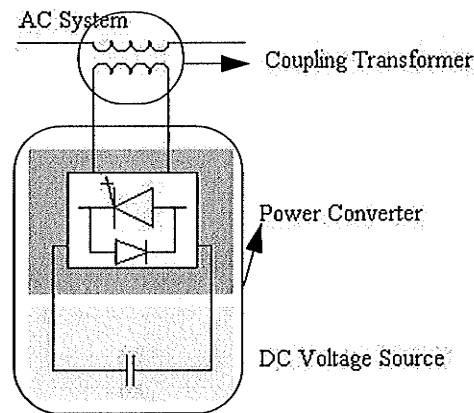


Fig. 2.7 Block Diagram of a SSSC

The SSSC injects a voltage into the power transmission line in quadrature to the line current, thus emulating an inductive or a capacitive reactance in series with the transmission line. The power flow on the transmission line can then be affected through the control of this series reactance.

Up to this point the devices were capable of supplying or absorbing reactive power in the power transmission system. However a new family of devices is obtained by combining the STATCOM and SSSCs. For instance UPFC combines a STATCOM and an SSSC. The Interline Power Flow Controller (IPFC) consists of two or more SSSCs. The Generalized Unified Power Flow Controller (GUPFC) uses a STATCOM and two or more SSSCs. The common feature of the devices mentioned is the possibility to exchange real power between their shunt and series components or between series components like in the IPFC.

Unlike STATCOM and SSSC devices which are only capable of providing reactive power, UPFC, IPFC and GUPFC have additional degrees of freedom as they allow for some real power exchange as well. These additional degrees of freedom are expected to result in greater flexibility and even allow for a better control of system stability through their rapid control actions [6], [11].

### **2.3.8 Unified Power Flow Controller (UPFC)**

SSSC is coupled to a STATCOM in a back-to-back arrangement. Thus, the shunt and series devices are able to exchange real power. This arrangement is called UPFC[5], [15]and it is illustrated in Fig 2.8. In this arrangement, the series device injects a voltage in series with the line without any restriction such as power system stability other than the device rating. In a widely used control concept, the shunt part is normally operated at unity power factor and is used to maintain constant voltage on the DC capacitor through the control of the real power. However one additional degree of freedom is available and may be used to generate or absorb reactive power at the shunt bus.

The first large scale practical demonstration of UPFC was installed at Inez Substation 138 kV located in eastern Kentucky in 1998. This project was a collaborative effort between American Electric Power (AEP), the Westing house Electric Corporation, and the Electric Power Research Institute (EPRI). UPFC comprises two  $\pm 160$  MVA Voltage Sourced Converters. The Power Converter of the three level type is shown in Fig 2.3. Each of the turn off capable valves in the converter counts of eight or nine 4000 A, 4.5 kV, GTO-Thyristors connected in series.

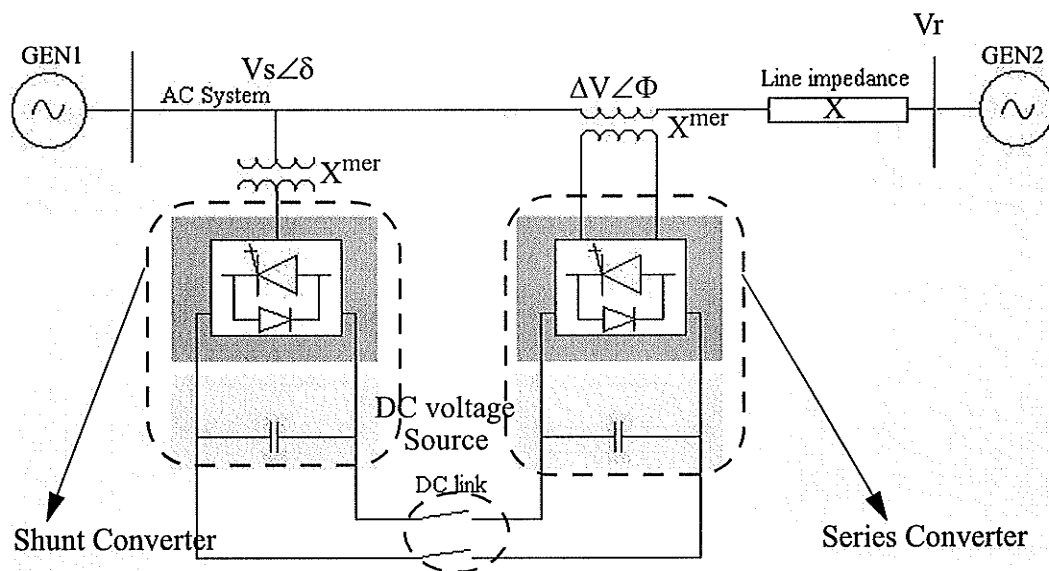


Fig. 2. 8 VSC Based Unified Power Flow Controller (UPFC).

In this chapter the basic concept of VSC based devices were presented. These devices employ self commutated DC to AC converters, using GTO or IGBT, to generate capacitive and inductive reactive power into AC transmission line and also exchange real power with the system.

In the section of the research that follows, we will investigate the system related various applications of VSC based devices such as UPFC and derive the mathematical framework of UPFC.

# CHAPTER 3 ANALYTICAL STUDIES OF TRADITIONAL POWER FLOW CONTROLLERS OF AN AC NETWORK

## 3.1 Simple point to point Power flow within an AC transmission network

Power flow within an AC transmission network as shown in Fig. 3.1 is dependent on transmission line Impedance ( $X$ ), the magnitude of  $V_s, V_r$ , and the phase angle ( $\delta$ ) between  $V_s$  and  $V_r$ .

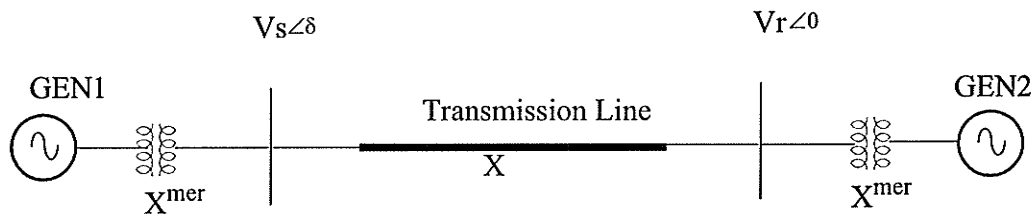


Fig. 3. 1 Simple AC Transmission Network

The transmitted uncompensated real power ( $P_o$ ) and reactive power ( $Q_o$ ) [3] flows of the above loss less transmission line (at the receiving end bus voltage) are given by the expressions:

$$P_o(\delta) = \frac{V_s V_r \sin(\delta)}{X} \quad (\text{EQ 3.1})$$

$$Q_o(\delta) = \frac{V_r(V_s \cos(\delta) - V_r)}{X} \quad (\text{EQ 3.2})$$

From the above two equations, we can see that the flow of  $P_o(\delta)$  and  $Q_o(\delta)$  can be controlled either by changing the power angle  $\delta$  or by changing line Impedance ( $X$ ) while keeping the Bus voltages constant.

#### **For the above AC transmission network system**

Assume  $V_s = V_r = V_{\text{base}}$

$$X = X_{\text{base}}$$

Considering above, we could convert transmission lines parameters in per unit (pu) [23] values which are as follows.

$$V_s = 1 \text{ pu}$$

$$V_r = 1 \text{ pu.}$$

$$\delta = 30^\circ \text{ deg}$$

$$X = 1 \text{ pu}$$

The transmitted  $P_o$  and  $Q_o$  at the receiving end are plotted against  $\delta$ . This can be seen in Fig 3.2. The reactive power as shown in Fig 3.3 is plotted against  $P_o$  within the stable value of phase angle  $\delta$  (i.e.  $0 \leq \delta < \pi$ )

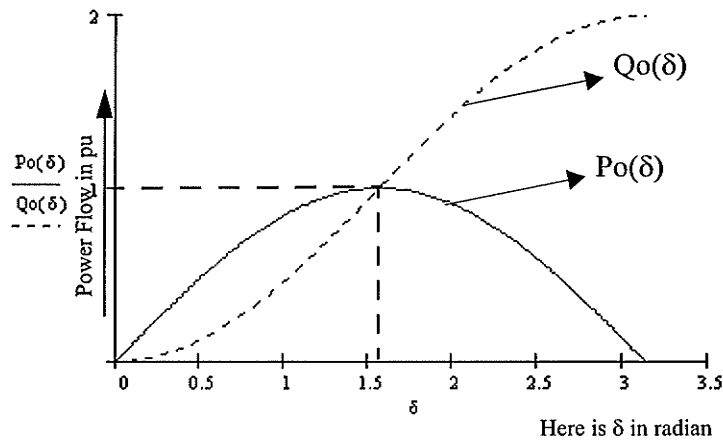


**Fig. 3. 2** Transmitted  $P_o(\delta)$  and  $Q_o(\delta)$  Versus Phase Angle

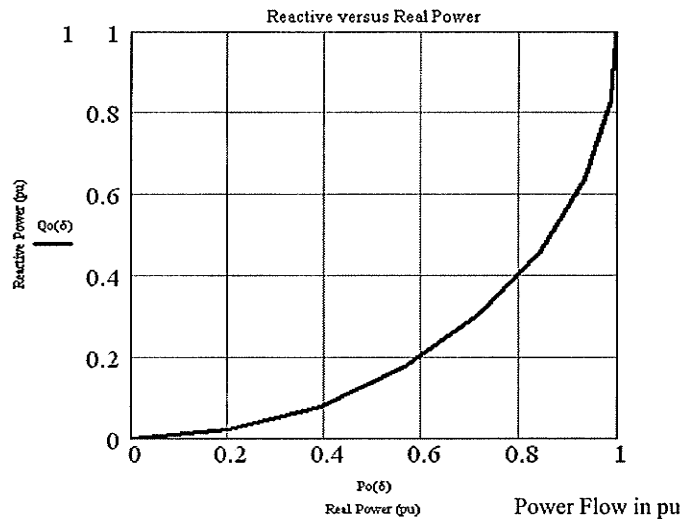


**Fig. 3. 3** Transmitted  $Q_o(\delta)$  Versus  $P_o(\delta)$  for  $\delta$  (i.e.  $0 \leq \delta < \pi/2$ )

From above two figures, we can conclude that the flow of real power of the transmission line is limited by the given transmission angle ( $\delta$ ). We also noticed that the real power ( $P(\delta)$ ) can't be changed without effecting the reactive power demand on the sending -and receiving -ends. A transmission line without high-speed control of system parameters

( $V_s, V_r, X$  and  $\delta$ ) can be utilized only to a level below maximum corresponding phase angle  $90^\circ$  due to power system stability constrain [24].

### **3.2 Traditional transmission line compensation and power flow control within AC transmission network**

The elementary equations (3.1) and (3.2) derived for the determination of  $P_o$  and  $Q_o$  show that any effort to increase real power transmission will inevitably result in an increase of reactive power demand on the end -voltage bus systems, and an increase of voltage variation along the transmission line. This hence plays a significant role in AC transmitted power flow control by providing the important functions of voltage regulations and reactive power management.

#### **3.2.1 Ideal MidPoint Shunt Compensator**

Consider the same AC transmission network model in which an ideal var compensator is shunt connected at the midpoint of the transmission line as shown in the Fig 3.4. This compensator is represented by a sinusoidal AC voltage source (of the fundamental frequency), in phase with the midpoint voltage, with an amplitude identical to that of the sending-and receiving-end voltages. The midpoint compensator [3] in effect segments the transmission line into two parts: the first segment, with an impedance of  $X/2$ , carries power from the sending end to the midpoint, and the second segment, also with an impedance with  $X/2$ , carries power from the midpoint to the receiving end. The midpoint var compensator exchanges only reactive power with the transmission line in this application.

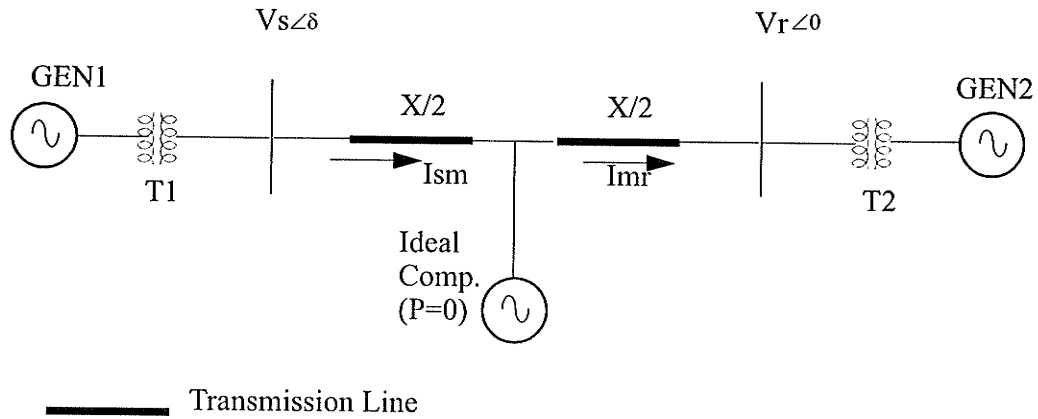


**Fig. 3. 4** AC Transmission Network with MidPoint Shunt Compensator

The relationship between voltages  $V_s$ ,  $V_r$ ,  $V_m$ , and the line segment currents  $I_{sm}$  and  $I_{mr}$  is shown by the phasor diagram in the Fig.3.5

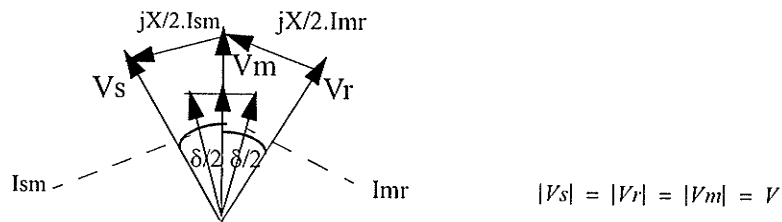


**Fig. 3. 5** Voltages and Currents Phasors of Shunt Compensator

The basic power flow given by equations (3.1) and (3.2) will be modified to equations (3.3) and (3.4), respectively, after considering addition of the midpoint shunt compensator [3] in the transmission network

$$P_c(\delta) = \frac{2 V_s V_r \sin\left(\frac{\delta}{2}\right)}{X} \quad (\text{EQ 3.3})$$

$$Q_c(\delta) = \frac{4 V_r \left( V_s \cos\left(\frac{\delta}{2}\right) - V_r \right)}{X} \quad (\text{EQ 3.4})$$

Here  $P_c$  and  $Q_c$  are compensated real and reactive power flows respectively.

The relationship between the compensated real ( $P_c(\delta)$ ) and reactive power ( $Q_c(\delta)$ ), and phase angle ( $\delta$ ) in the case of midpoint shunt compensator is plotted in Fig. 3.6. It can be observed that the midpoint shunt compensation can significantly increase the transmittable power (doubling uncompensated real power ( $P_o$ ) value at  $\delta=180^\circ$ ) at the expense of rapidly increasing reactive power demand on the mid point compensator.

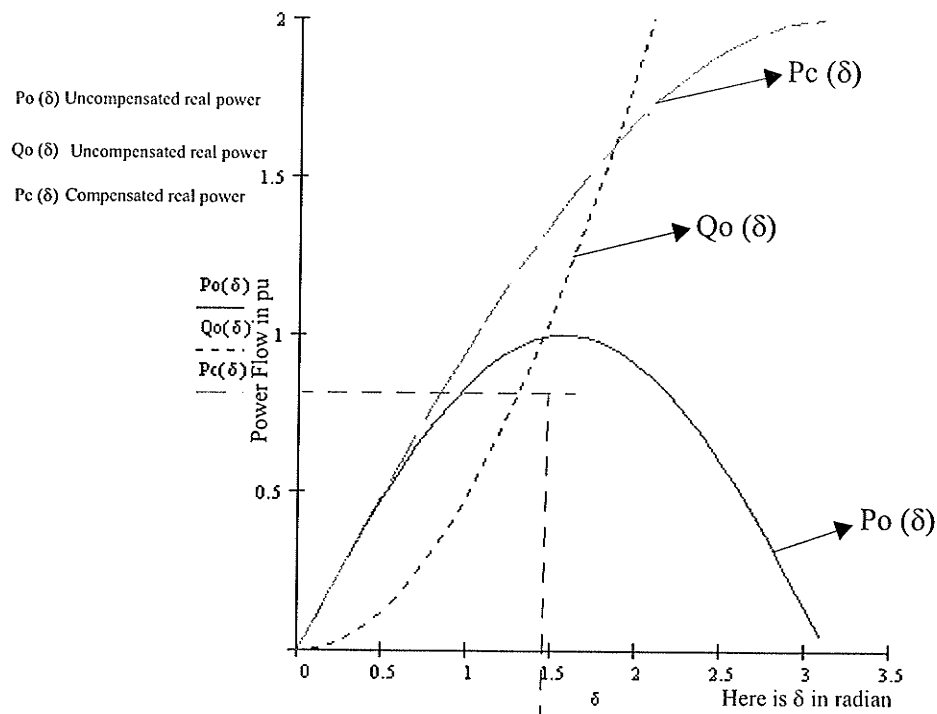


Fig. 3. 6 Real & Reactive Power Versus Power Angle ( $\delta$ )

This midpoint shunt compensator (mechanical -switched capacitors) is very useful to control transmission line voltage where there are slow, daily and seasonal load variations. At the same time, midpoint shunt compensator provides economical solutions to steady- state transmission problems. However midpoint shunt compensator's limited operating speed makes it largely ineffective under dynamic system conditions. In addition to this, there is a limitation to the number of switching operations permitted. Therefore midpoint shunt compensator lacks the flexibility of operation which is required by a modern power system. However, a STATCOM or SVC has adequate operating speed.

### **3.2.2 Series Compensation**

The philosophy behind series compensation is to decrease the overall effective series transmission impedance ( $X$ ) from the sending-end. The conventional view is that the impedance of the series connected compensating capacitor cancels a portion of the actual line reactance and thereby the effective transmission impedance is reduced as if the line was physically shortened. An equally valid physical view is that, in order to increase the transmitted power, the voltage across the series impedance has to be increased. This can be accomplished by a series connected circuit element [6] that produces a voltage opposite to the prevailing voltage across the series line reactance. The simplest element to achieve the purpose is a capacitor.

Consider the same AC transmission network with a series capacitor as shown in Fig 3.7.

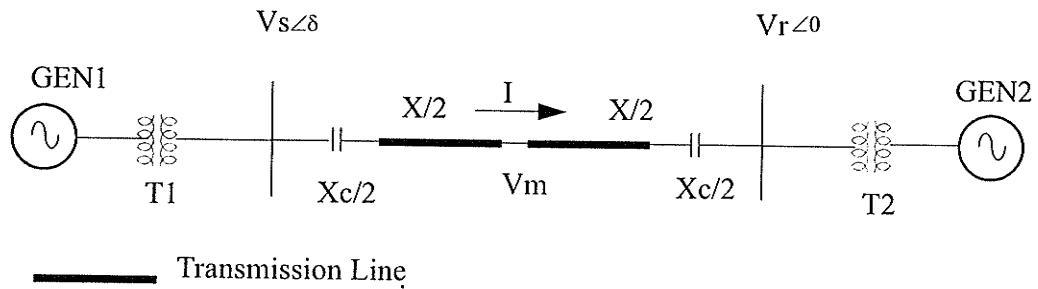


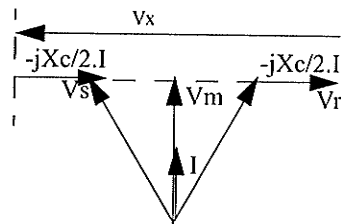
**Fig. 3. 7** AC Transmission Network with Series Compensation

Here the transmission line effective reactance is  $X - X_c$  instead of  $X$ .

$$X_{eff} = X - X_c$$

$$X_{eff} = X(1 - K) \quad \text{where } K = X_c/X, \quad 0 < K < 1, \text{ the degree of series compensation.}$$

The relationship between voltages  $V_s$ ,  $V_r$ ,  $V_m$  and the line segment current  $I$  is shown by the phasor diagram in the Fig.3.8



$V_x$  is total voltage drop across the line inductance

**Fig. 3. 8** Current and Voltage Phasors for Series Compensation

The derivation of the real power transmitted through this line is as follows:

$$I = \frac{2VSin\left(\frac{\delta}{2}\right)}{X(1 - K)} \quad \text{(EQ 3.5)}$$

The real power transmitted for the above system can be given by following equation:

$$P_c(\delta, K) = \frac{V_s V_r \sin(\delta)}{X(1-K)} \quad (\text{EQ 3.6})$$

And the reactive power supplied by the capacitor is given by equation no. (3.7)

$$Q_c(\delta, K) = \frac{2V_r \left( V_s \cos\left(\frac{\delta}{2}\right) - V_r \right)}{X(1-K)^2} K \quad (\text{EQ 3.7})$$

From the above two equations, we could establish the relationship between the real power ( $P_c(\delta, K)$ ), series capacitive reactive power ( $Q_c(\delta, K)$ ), and phase angle  $\delta$  as shown in the Fig 3.9.

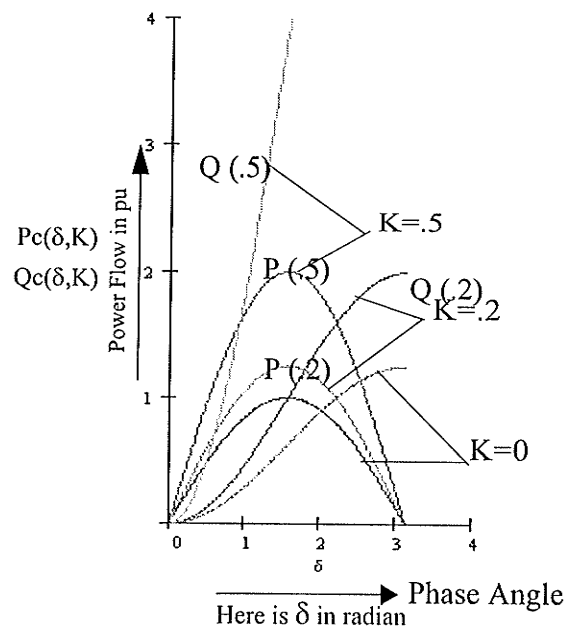


**Fig. 3.9** Real and Reactive Power Versus Phase Angle  $\delta$

It can be observed that, as expected, the series compensation can significantly increase the transmittable power (doubling uncompensated real power ( $P_0$ ) value at  $K=.5$  for  $\delta = 90^\circ$ )

with the degree of series compensation  $K$ . Similar to this, the reactive power (four times the uncompensated reactive power ( $Q_0$ ) value at  $K = 0.5$  for  $\delta = 90^\circ$ ) also increases by reducing  $K$ .

### Application

Series compensators have been used in power system to enhance the stability and loadability of AC transmission lines.

#### 3.2.3 Phase Angle Control (PAR):

The basic concept of the phase angle regulation [4] is an addition of an appropriate quadrature component to the sending-and/or prevailing, terminal (bus) voltage in order to change (increase or decrease) sending end phase angle to the desired value. Thus PAR controls the flow of power in the transmission line.

Consider the same AC network model with Phase Angle Regulator inserted between the sending-end voltage and the transmission line as shown in the Fig. 3.10.

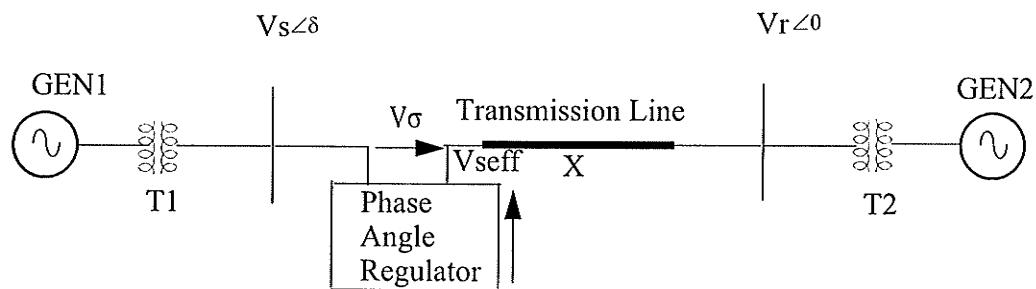
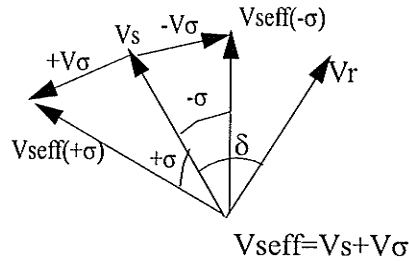


Fig. 3. 10 AC Transmission Network with PAR

Theoretically, the PAR can be considered as a sinusoidal (fundamental frequency) AC voltage source with controllable amplitude ( $V_\sigma$ ) and phase angle ( $\sigma$ ). For an Ideal phase angle

regulator, the angle of phasor  $V_{\sigma}$  relative to phasor  $V_s$  is stipulated to vary with  $\sigma$  so that the angular change does not result in a magnitude change. This can be seen in the phasor diagram given by Fig 3.11.



**Fig. 3. 11** Current and Voltage Phasors of PAR

The relationship between the real power ( $P$ ) and reactive power ( $Q$ ) with phase angles  $\delta$  and  $\sigma$  are given by equations (3.8) and (3.9) respectively and is also plotted in Fig. 3.12. It can be seen that the phase angle regulator does not increase the transmittable power of the uncompensated line, However PAR makes theoretically possible to keep the power at its maximum value at any angle  $\delta$  in the range of  $(\pi/2-\sigma)$  to  $(\pi/2+\sigma)$  by shifting the  $P$  Versus.  $\delta$  curve to the right or left to provide optimal loading of the transmission lines.

$$P(\delta, \sigma) = \frac{V_s V_r \sin(\delta \pm \sigma)}{X} \quad (\text{EQ 3.8})$$

$$Q_c(\delta, \sigma) = \frac{V_r (V_s \cos(\delta - \sigma) - V_r)}{X} \quad (\text{EQ 3.9})$$

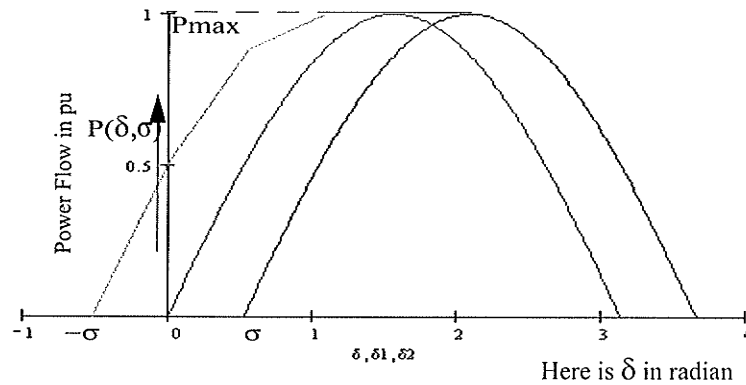


Fig. 3. 12 Real Power Versus Phase Angle ( $\delta$ )

### Application

PAR employing a shunt connected excitation transformer with a mechanical tap changer and a series inserted transformer is often connected to the transmission line to control steady state power flow and prevent undesirable loop power flows.

### 3.3 Summary

The traditional reactive power compensators such as shunt and series can significantly increase the steady state maximum transmittable power flow in the transmission lines. However their response time in supporting a power system is not fast enough due to the inherent inertia of mechanical switches operating device.

Due to this limitation, It was decided to study the capabilities of suitable and fast acting power electronic devices such as UPFC[5]. This will be discussed in the next chapter.

## CHAPTER 4      MATHEMATICAL MODEL OF UPFC.

---

### 4.1    Power flow of a transmission line with UPFC

#### Basic Concepts

UPFC is a combination of Static Synchronous (Shunt part) and Static Series Compensators (Series part) which are coupled together via a common DC link (Capacitor) to allow bidirectional flow of real power between the series and shunt converter output terminals and to provide real and reactive line compensation without an external energy source. UPFC by means of angularly unconstrained series voltage injection ( $\Delta V \angle \Phi$ ) is able to control, concurrently or selectively, the transmission line sending end voltage ( $V_s$ ) [5],[16].

As shown in the Fig 4.1, the point to point AC transmission network is extended to include UPFC.

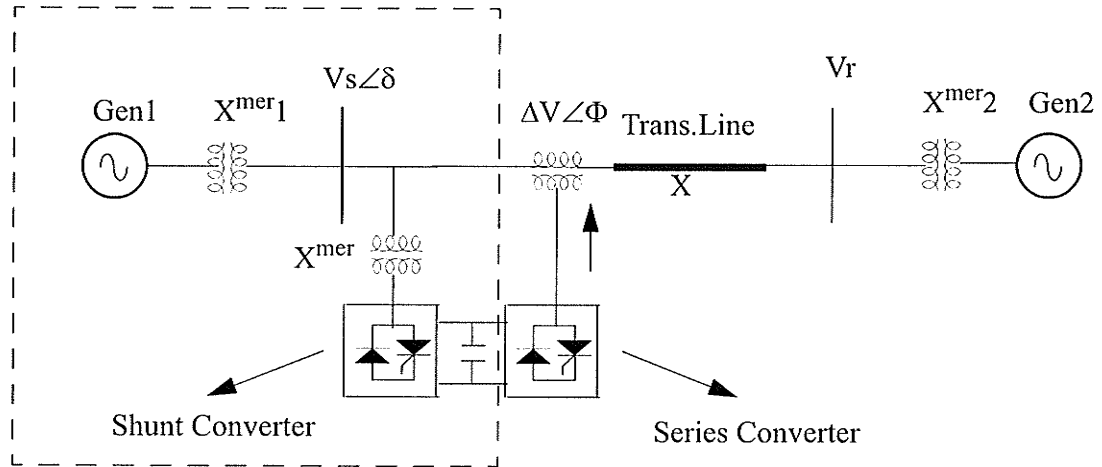


Fig. 4. 1 AC Transmission Network with UPFC

The voltage injected by SSSC in series with a transmission line is represented by a phasor  $\Delta V \angle \Phi$  having magnitude of  $\Delta V$  where the limits are  $-.5 \leq \Delta V \leq .5$  pu (due to the cost constraint of the devices) and angle  $\angle \Phi$  ( $0^\circ \leq \Phi \leq 360^\circ$ ). This voltage can be vectorially added to the sending end voltage ( $V_s \angle \delta$ ) as shown by the Fig.4.1. It can be seen that the transmission line “sees”  $V_s + \Delta V \angle \Phi$  is the effective sending end voltage ( $V_{seff}$ ). Thus it is clear that UPFC affects the voltage (both its magnitude and phase angle) across the transmission line, and therefore it is reasonable to expect its ability to control, by varying the magnitude and phase angle of the transmittable real as well as reactive power demand of the line at any given transmission phase angle between the sending and receiving end voltages. The real and reactive power flow at the receiving end of the loss less transmission line with UPFC is given by following equations (4.1) and (4.2).

Real power with UPFC:

$$P(\delta, \phi) = \frac{V_s V_r \sin(\delta) + \Delta V V_r \sin(\phi)}{X} \quad (\text{EQ 4.1})$$

from equation (3.1) and (4.1)

$$P(\delta, \phi) = P_o(\delta) + \frac{\Delta V V_r \sin(\phi)}{X} \quad (\text{EQ 4.2})$$

$$\Delta V \sin(\phi) = \frac{P(\delta, \phi) - P_o(\delta) \times X}{V_r} \quad (\text{EQ 4.3})$$

Reactive Power with UPFC

$$Q(\delta, \phi) = \frac{V_r (V_s \cos(\delta) + \Delta V \cos(\phi)) - V_r^2}{X} \quad (\text{EQ 4.4})$$

from equation (3.2) and (4.4)

$$Q(\delta, \phi) = Q_o(\delta) + \frac{V_r \Delta V \cos(\phi)}{X} \quad (\text{EQ 4.5})$$

$$\Delta V \cos(\phi) = (Q(\delta, \phi) - Q_o) \frac{X}{V_r} \quad (\text{EQ 4.6})$$

from equation (4.3) and (4.6), the magnitude and phase angle of the voltage injected in series with the transmission line to provide the required real and reactive power are given by following equations:

$$\Delta V = \frac{X}{V_r} \sqrt{(Q(\delta, \phi) - Q_o)^2 + (P(\delta, \phi) - P_o)^2} \quad (\text{EQ 4.7})$$

Phase angle of injected voltage

$$\phi = \text{atan} \left( \frac{P(\delta, \phi) - P_o}{Q(\delta, \phi) - Q_o} \right) \quad (\text{EQ 4.8})$$

The above equations give us information about  $\Delta V$  and phase angle  $\Phi$  which we have to inject in series with the transmission line to get the demanded real and reactive power by the system within the specified range defined by the maximum limit of injected  $\Delta V$ . The design of control scheme based on above equations is discussed later in this chapters (Fig 4.3).

Based on the above mathematical derivation, we could come up with a phasor diagram [1],[2], as shown in Fig.4.2, which gives the magnitude and phase angle of injected voltage to meet the demand of real and reactive power of the power system. The range to control the real and reactive power will be specified by the maximum limit of injected  $\Delta V$ .

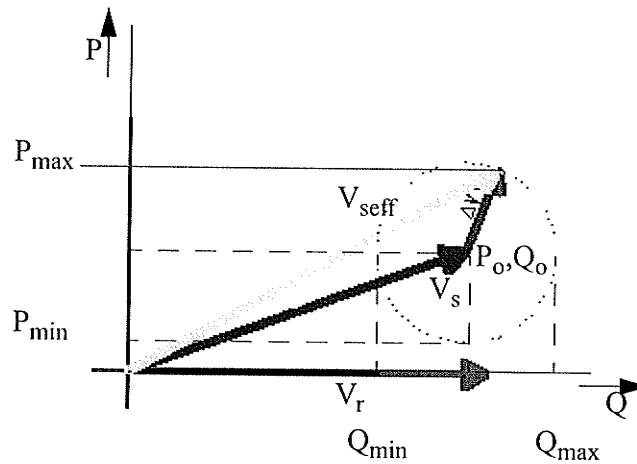


**Fig. 4. 2** Range of Transmittable Power Versus Phase Angle ( $\delta$ ) of a UPFC

From the above discussion, we can conclude that the real power ( $P$ ) and the reactive power at the receiving end ( $Q$ ) can be controlled between

$$P_o(\delta) - \frac{\Delta V_{max}}{X} \leq P(\delta, \phi) \leq P_o(\delta) + \frac{\Delta V_{max}}{X} \tag{EQ 4.9}$$

$$Q_o(\delta) - \frac{\Delta V_{max}}{X} \leq Q(\delta, \phi) \leq Q_o(\delta) + \frac{\Delta V_{max}}{X} \tag{EQ 4.10}$$

at any transmission angle ( $\delta$ ).

As shown in the Fig 4.3 and Fig 4.4, the wide range of control for the transmitted power which is independent of the transmission angle ( $\delta$ ) indicates not only superior capability of UPFC in power flow applications, but also promises powerful capacity for transient stability improvement and power oscillation damping [17],[18].

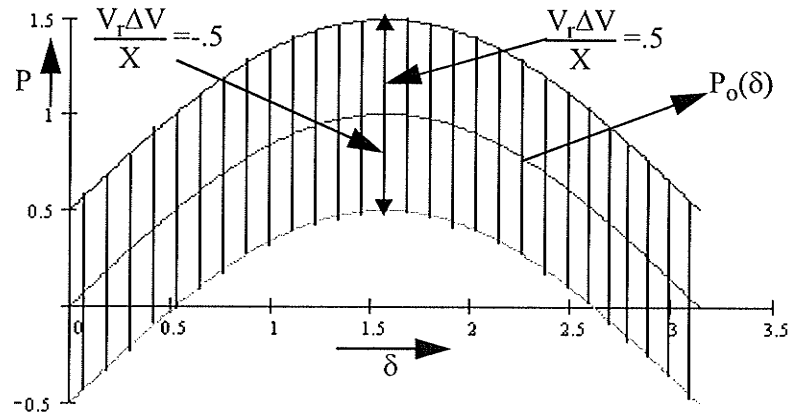


Fig. 4. 3 Range of Transmittable Real Power (P) Versus Angle ( $\delta$ ) of a UPFC

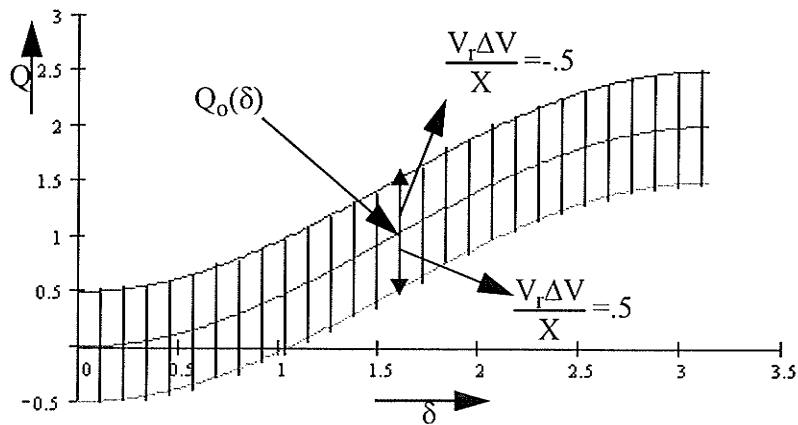


Fig. 4. 4 Range of Transmittable Reactive Power (Q) Versus Angle ( $\delta$ ) of a UPFC

As seen from Fig 4.3 and 4.4, The range of transmitted real and reactive power, at any given transmission angle ( $\delta$ ) within power system stability limit, of the above discussed UPFC offers superiority ( $\pm 0.5$  pu) over the range of uncompensated AC transmission line given by Fig 3.2 and 3.3.

The powerful capabilities of UPFC discussed above in terms of conventional transmission control concepts can be integrated into a generalized power flow controller that is able to maintain prescribed, and independent controllable, real power and reactive power  $Q$  in the line [5].

#### 4.2 Independent Control of Real and Reactive Power Flow

Considering the equations (4.7) and (4.8), we notice that the real and reactive power changes from the uncompensated values,  $P_o(\delta)$  and  $Q_o(\delta)$ , as a function of the magnitude and phase angle of the injected voltage  $\Delta V$ . Since the angle  $\Phi$  is an unrestricted variable ( $0 \leq \Phi \leq 360^\circ$ ), the boundary of the attainable control region [3] for  $P(\delta, \Phi)$  and  $Q(\delta, \Phi)$  is obtained from a complete rotation of the phasor  $\Delta V$  with its maximum  $\Delta V_{max}$ . The above mentioned equations confirm that this control region is a circle with a center defined defined by the coordinates defined by  $P_o(\delta)$  and  $Q_o(\delta)$  and the radius is given by following equation:

$$(P(\delta, \phi) - P_o(\delta))^2 + (Q(\delta, \phi) - Q_o)^2 = \left(\frac{\Delta V}{X}\right)^2 \quad (\text{EQ 4.11})$$

Equation(4.11) defines the circular control regions which are shown in Fig 4.5 for the same system detail as discussed earlier for the conventional methods ( $V_s=1$  pu,  $V_r= 1$  pu

and  $X=1$  pu and the injected voltage magnitude  $\Delta V=0.5$  pu). The centers of these circles (indicated by + sign) are  $P_o(\delta)$ ,  $Q_o(\delta)$  at angles  $\delta=0^\circ$ ,  $\delta=30^\circ$ ,  $\delta=60^\circ$  and  $\delta=90^\circ$  respectively. The locus of the centers are indicated by the + sign as  $\delta$  varies between  $0^\circ$  and  $90^\circ$ .

The Fig.4.5 illustrates the case when the transmission line angle ( $\delta$ ) is zero with  $\Delta V=0$ ,  $P_o(\delta)$  and  $Q_o(\delta)$  are zero i.e. the system is at standstill at the origin of the P and Q coordinates. The circle around the origin of the plane is the loci of the corresponding Q (at receiving end), and P values, obtained as the voltage phasor  $\Delta V$  is rotated a full revolution ( $0 \leq \Phi \leq 360^\circ$ ) with its maximum value  $\Delta V_{max}$ .

The circle in the [P,Q] plane shows all P and Q values attainable with UPFC of a given rating. As we can see from the Fig. 4.5 and Fig. 4.6, UPFC with the stipulated voltage rating of 0.5 pu is able to establish 0.5 pu power flowing into either directions, without imposing any additional reactive power demanded on either the sending or the receiving end bus.

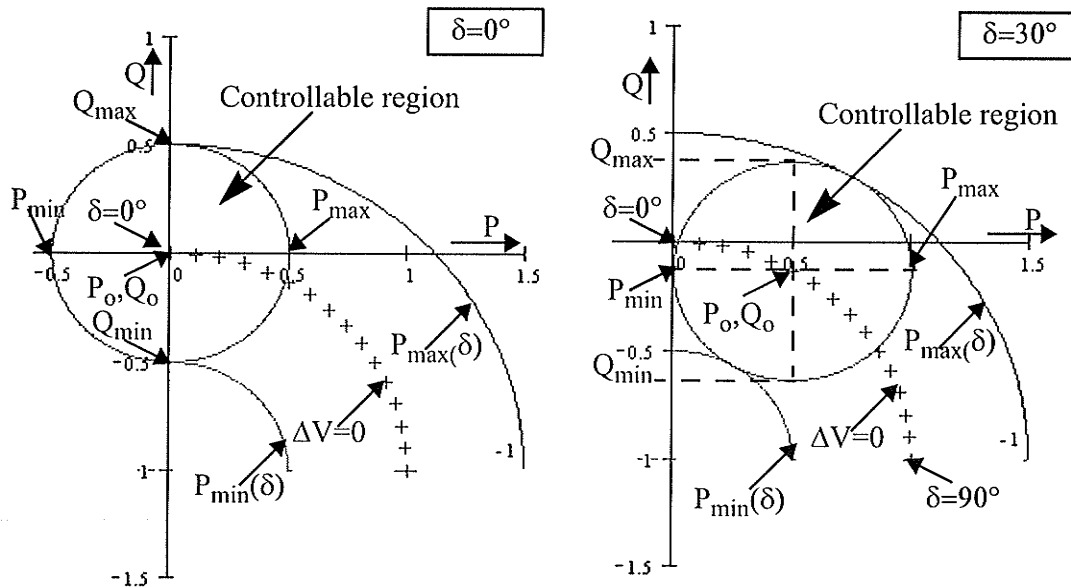


**Fig. 4. 5** Control Region of Attainable Real Power and Reactive Power with a UPFC for  $\delta=0^\circ$  &  $\delta=30^\circ$

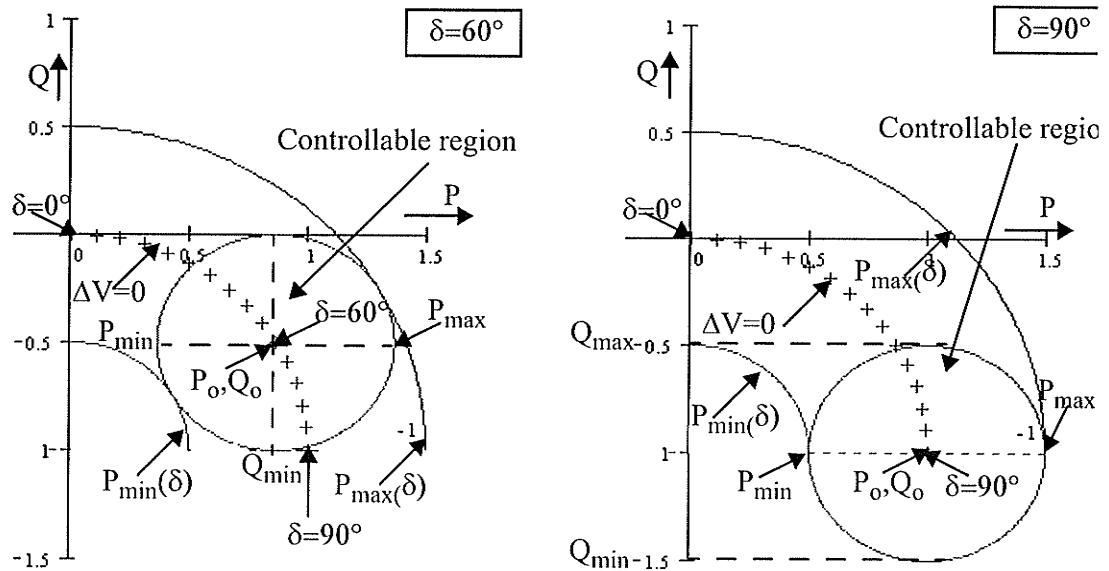


Fig. 4. 6 Control Region of Attainable Real Power and Reactive Power with UPFC for  $\delta=60^\circ$  &  $\delta=90^\circ$

Figs 4.5 and 4.6 demonstrate that UPFC, with its unique capability to control independently the real and reactive power flow at any transmission angle, provides a powerful tool for AC transmission control [3].

### 4.3 Control methods of UPFC

The exceptional operating characteristics of UPFC are due to its unique ability to inject an AC compensating voltage vector  $\Delta V \angle \Phi$  with arbitrary magnitude and angle in series with the transmission line within specified equipment's maximum rating limits.

Considering that UPFC is a combination of Shunt and Series Converters which are coupled via a common DC link(Capacitor), control methods [18],[19] are studied for both the converters individually.

### 4.3.1 Control Methods of Shunt Converter

The shunt converter which is also called as STATCOM [9] is operated to draw a controlled current from the transmission line for the following reasons;

- To maintain the transmission line voltage to a reference value at the point of connection by providing or absorbing reactive power.
- To maintain a preset DC voltage level on the DC link.

#### Reactive Power Control Method

To understand the method of controlling of reactive power component of a Shunt Converter, we could assume that there is no net exchange of real power in the steady state. Hence the DC source can be replaced by a capacitor, as shown by Fig. 4.7. Also, in perfectly balanced conditions, the energy storage requirement for this capacitor is very small because the instantaneous real power in each phase is provided by the other two via STATCOM's switching actions. Hence, the role of the capacitor is to provide energy storage during transients and unbalanced operation and also to provide the reactive power at the DC harmonic frequencies.

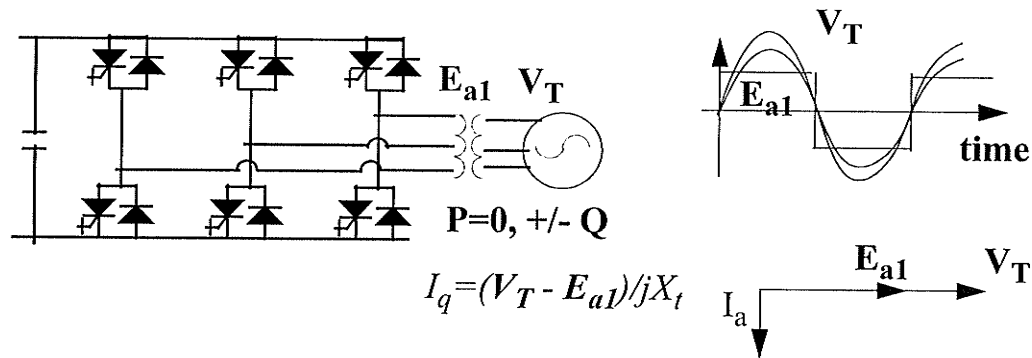
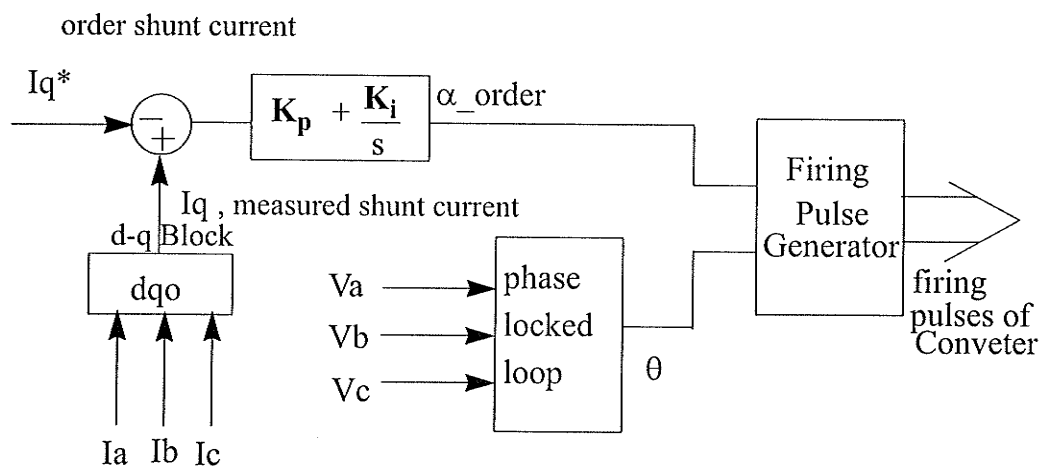


Fig. 4. 7 Basic Principal of Shunt Converter Operation

The value of the reactive current entering the Shunt Converter shown by Fig 4.7 is given by

$$I_q = \frac{(V_T - E_{a1})}{jX_t} \tag{EQ 4.12}$$

where  $V_T$  is magnitude of the AC side voltage,  $E_{a1}$  the fundamental component of the switched voltage (directly proportional to the DC bus voltage) on the valve side of the transformer and  $X_t$  is the reactance of the Shunt Converter transformer. Here we have transformed the circuit to the AC network side so that the turns ratio does not appear in the calculations. As the firing of the Shunt Converter valves is carried out at a firing angle of  $0^\circ$ , so as to provide an output that is in phase with the system voltage, the steady-state real current is zero. However, if the firing of the valves is momentarily advanced, then  $E_{a1}$  would lead  $V_T$  and energy would be transferred from the capacitor into the AC network, thereby reducing the capacitor DC voltage. The opposite happens when the firing is retarded from its steady state value. The firing angle reverts to zero when the appropriate voltage is reached to provide the desired reactive power. This momentary deviation of the firing angle is one of the techniques used in Shunt Converter for controlling the reactive power. Thus, a typical lowest-level control system for the Shunt Converter based on this approach is shown in the Fig.4.8 below:



**Fig. 4. 8** Simple Control System for Shunt Converter

In the above control system, the reactive current order ( $I_q^*$ ) is compared with the actual reactive current ( $I_q$ ) and the firing angle ( $\alpha$ ) suitably changed via a proportional-integral control system. The angle is in phase with the positive sequence of the fundamental AC waveform and is generated using a phase-locked loop which is locked to the AC system voltages. The component  $I_q$  can then readily be calculated using the Park Transformation:

$$\begin{bmatrix} i_d \\ i_q \\ i_0 \end{bmatrix} = \frac{2}{3} \begin{bmatrix} \cos(\theta) & \cos\left(\theta - \frac{2}{3}\pi\right) & \cos\left(\theta + \frac{2}{3}\pi\right) \\ \sin(\theta) & \sin\left(\theta - \frac{2}{3}\pi\right) & \sin\left(\theta + \frac{2}{3}\pi\right) \\ \frac{1}{2} & \frac{1}{2} & \frac{1}{2} \end{bmatrix} \begin{bmatrix} i_a \\ i_b \\ i_c \end{bmatrix} \quad (\text{EQ 4.13})$$

Where  $i_a$ ,  $i_b$  and  $i_c$  are line side currents.

**Reactive Power Control Method With Constant DC Voltage**

It must be realized that the charging/discharging of the capacitor voltage can increase the transient response time, particularly with a large value of capacitance as would be the case for a Shunt Converter designed to work with large unbalances. Hence it is sometimes desired, especially for STATCOM's designed for use at the sub-transmission/distribution level that the reactive power be variable without a variation in the DC bus voltage.

In the PWM STATCOM [9], we can regulate the reactive power (current) from a line without affecting the DC voltage with the help of using two closed loop control methods.

Because the output voltage can be controlled by using Sinusoidal Pulse Width Modulation (SPWM) controller and selecting the proper modulation index. Thus an arrangement with SPWM controller (Appendix A) as shown in Fig. 4.9 is possible.

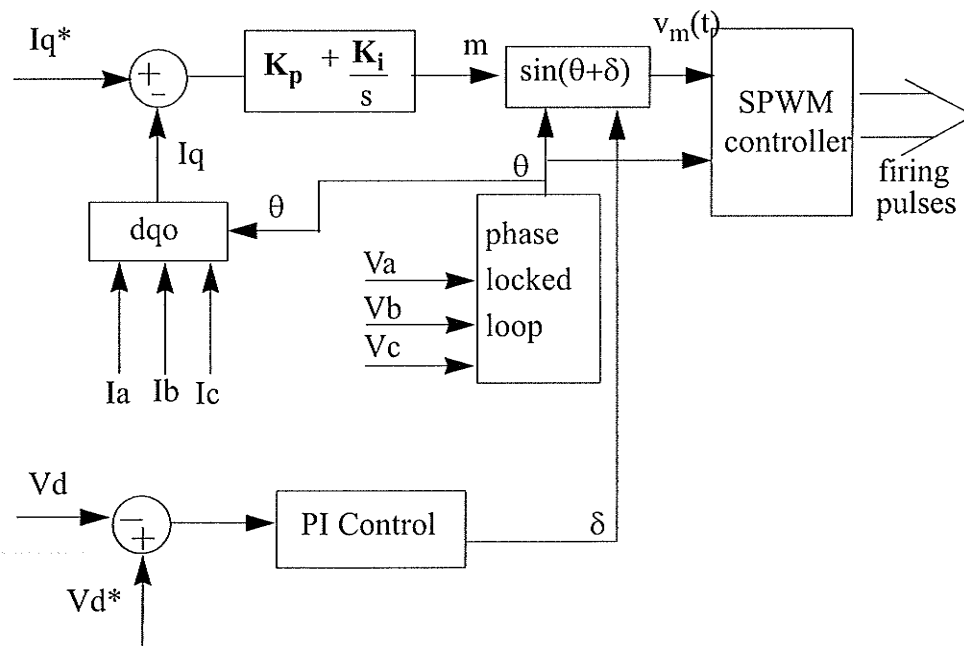


**Fig. 4. 9** Control Blocks for PWM Shunt Converter

---

In this arrangement, the DC capacitor voltage is controlled via the phase angle  $\delta$  between the AC side voltage and fundamental component of the switched voltage on the valve side of the transformer. Because changing the capacitor voltage requires a transfer of real power to, or from the DC bus which can only be achieved by introducing a phase shift between the Shunt Converter and AC system voltages.

However, it can be seen from Fig 4.9 that this arrangement has a drawback that the two control loops are not decoupled because a change in DC voltage via the parameter  $\delta$  would also immediately affect the reactive component and thus the control loops require a change in the output (m) of the first loop in order to keep  $I_q$  at its setpoint. Decoupling of the two loops may be achieved by synthesizing the proper signal voltage as shown in Fig. 4.10.

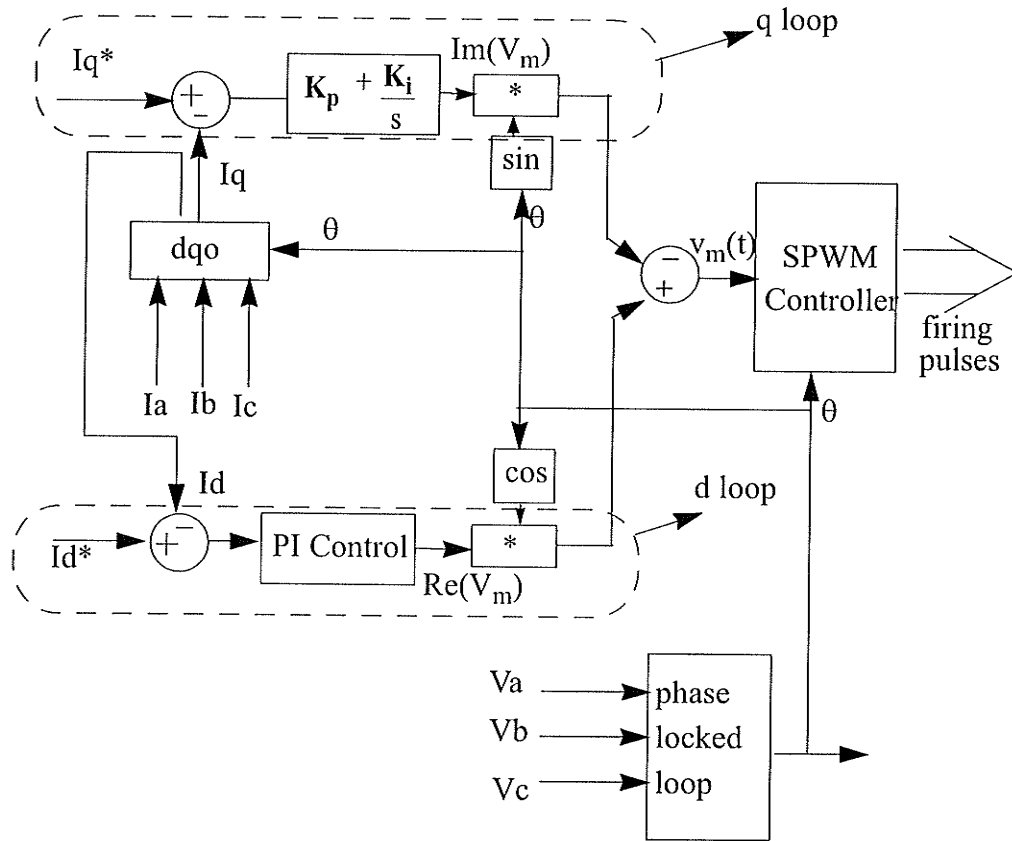


Fig. 4.10 Control Circuit for PWM STATCOM with steady state de-coupling loops

If the AC line is considered to be a pure reactance with no losses, Equations (4.3) and (4.6) indicate a method to make a decoupled controller in which the order real power  $P^*$  do not affect the reactive power  $Q^*$  and vice-versa. Using complex notation, the quantities  $\Delta V \cos(\phi)$  and  $\Delta V \sin(\phi)$  can be considered as real (direct axis) and imaginary (quadrature axis) components of the injected voltage vector. It can be seen from Equations 4.3 and 4.6 that the q component of the injected voltage affects only the real power flow and the d component the imaginary power. Thus we can introduce two control loops, each affecting only the d, or the q component. The desired injected voltage waveform, as shown in the Fig. 4.10, can then be generated by multiplying the control signal of the d loop by  $\cos(\theta)$

and the q loop by  $\sin(\theta)$  and then summing the two products. The signal  $\cos(\theta)$  or  $\sin(\theta)$  can be obtained from a phase-locked loop (PLL) which tracks the voltage of the sending end busbar.

In above case, although the d and q loops are steady state independent, there is still transient coupling which will be discussed in the chapter 5 (modeling stage).

Other control aspects at this level of control not shown in the control diagram include:

- transformer saturation control (control of DC side system current)
- voltage balance control if several capacitors are present as in a multi-level STATCOM
- Converter AC current and DC capacitor voltage limits.

#### 4.3.2 Control Methods of Series Converter

The series converter controls the magnitude and phase angle of the injected voltage in series with the transmission line to provide the desired real and reactive power flow in the transmission line.

Control methods are mainly studied for the following reason;

- To provide independent control for real and reactive power flow in the transmission line.

#### Open-Loop Control Method

Equations. (4.7) and (4.8) can be used to determine the magnitude and the phase angle of the injected voltage ( $\Delta V \cos(\omega t + \phi)$ ) for any desirable real  $P^*$  and reactive power order  $Q^*$ , respectively. However, this control scheme requires a foreknowledge of the uncompen-

sated real and reactive power flow,  $P_o$  and  $Q_o$ , respectively, as well as the receiving end voltage  $V_r$ . A control method based on Open-Loop Control with slow feedback adjustment, as shown in the Fig.4.11, has been studied on this project

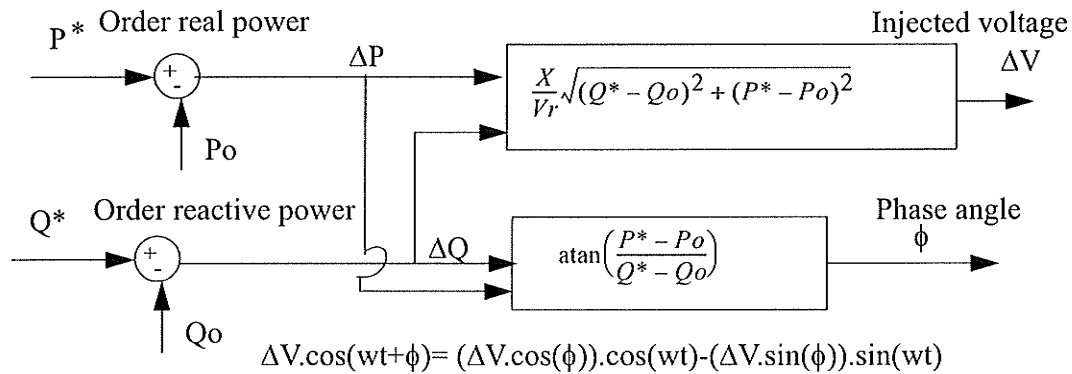


Fig. 4. 11a Open-Loop Control of a Series Converter

The above scheme ensures that the bulk of the ordered real ( $P^*$ ) and reactive ( $Q^*$ ) power are achieved with an open-loop response.

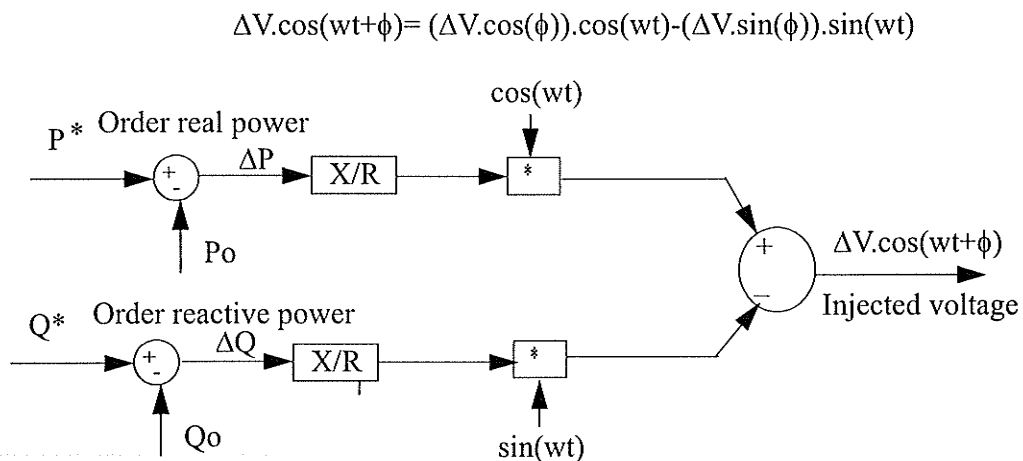


Fig. 4. 11b Equivalent Representation of Rectangular Coordinates

To compensate for uncertainties in the knowledge of uncompensated real and reactive power flow,  $P_o$  and  $Q_o$ , respectively, and also transmission line impedance  $X$  and receiving end voltage  $V_r$ , the above slow feedback loop can be modified as shown in the Fig 4.11.

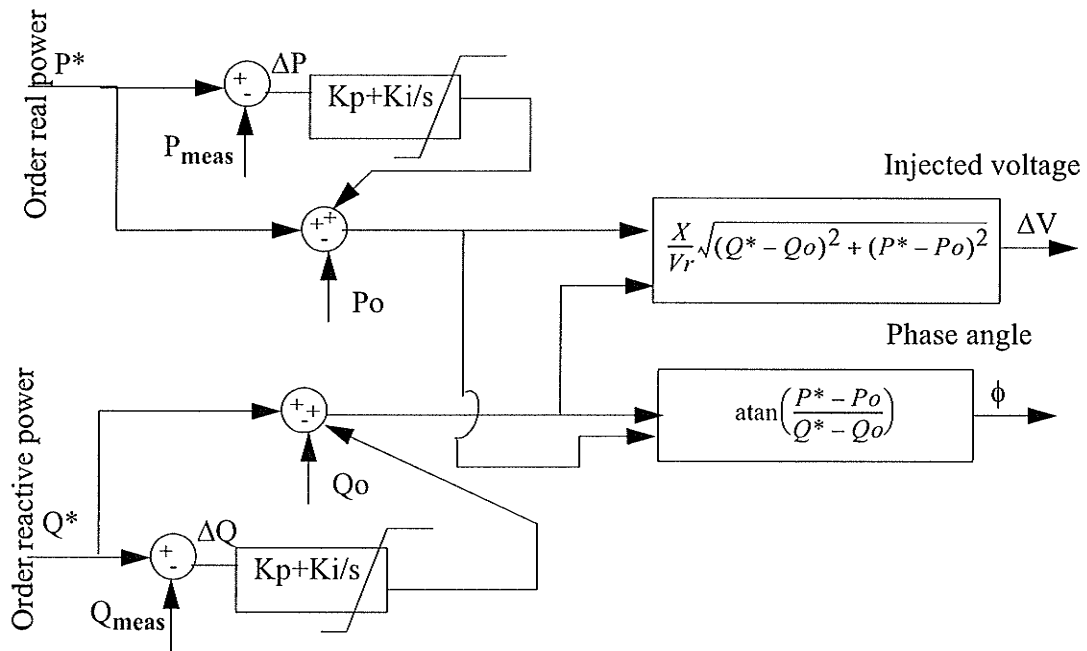


Fig. 4. 12 Slow Feedback Loop with Main Open-Loop Control

As shown in the Fig 4.12, an error signal is generated between ordered and measured values of real power  $P$  and reactive power  $Q$  which can be passed through a proportional-integral (PI) controller and summed with the requested real power  $P^*$  and reactive power  $Q^*$ , and then passes through injected voltage and phase angle blocks to generate required injected voltage.

Note: This control action ceases only when the ordered and measured powers are equal.

**Control Method Based on d-q Components**

If the AC line is considered to be a pure reactance with no losses, Equations (4.3) and (4.6) indicate a method to make a decoupled controller in which the order real power  $P^*$  do not affect the reactive power  $Q^*$  and vice-versa. Using complex notation, the quantity  $\Delta V \cos(\phi)$  and  $\Delta V \sin(\phi)$  can be considered as the real (direct axis) and imaginary (quadrature axis) components of the injected voltage vector. It can be seen from Equations (4.3) and (4.6) that the q component of the injected voltage affects only the real power flow and the d component the imaginary power. Thus we can introduce two control loops, each affecting only the d, or the q component. The desired injected voltage waveform, as shown in the Fig. 4.13, can then be generated by multiplying the control signal of the d loop by  $\cos(\omega t)$  and the q loop by  $\sin(\omega t)$  and then summing the two products. The signal  $\cos(\omega t)$  or  $\sin(\omega t)$  can be obtained from a PLL which tracks the voltage of the sending end busbar.

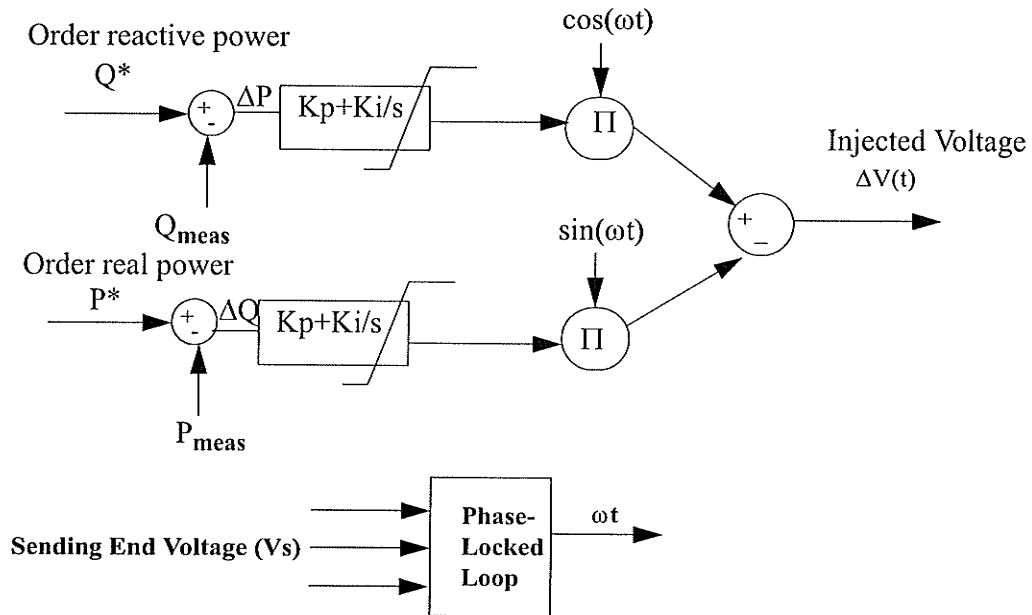


**Fig. 4. 13** Closed Loop Partially Decoupled Control

**Decoupled Control Method based on d-q axis**

As we learnt that in the case of a series UPFC branch, the real and reactive power flows in the transmission line are influenced by the magnitude as well as the phase angle of the series injected voltage. Therefore, the real power controller can significantly affect the level of reactive power flow and vice versa. In order to improve the performance and reduce the interaction between the real and reactive power control, a so-called decoupled watt-var control algorithm based on d-q axis theory was used [20],[21],[22].

It can be shown [20],[22] that with line resistance included, the mathematical model for the response of a Voltage Sourced Converter to an applied voltage  $V = vd$  into a synchronously rotating orthogonal system can be given as

$$\frac{d}{dt} \begin{bmatrix} id \\ iq \end{bmatrix} = \begin{bmatrix} \frac{R}{L} & \omega \\ -\omega & \frac{R}{L} \end{bmatrix} \begin{bmatrix} id \\ iq \end{bmatrix} + \frac{1}{L} \begin{bmatrix} vd - ed \\ -eq \end{bmatrix} \tag{EQ 4.14}$$

Here, the AC busbar voltage is taken as reference and thus only has a real component  $vd$ . Voltages  $ed$  and  $eq$  are the d and q components of the injected voltage of VSC; L and R are the line inductance and resistance respectively.

Both d-q axis components of the current are cross-coupled through the term  $\omega$ .

For the purposes of further derivation of the new control system, the classical decoupled watt-var algorithm [20] was studied. By interdicting two new variables  $x1$  and  $x2$

$$x1 = \frac{vd - ed}{L} \quad \text{and} \quad x2 = \frac{-eq}{L} \tag{EQ 4.15}$$

Equation (4.14) leads to the following mathematical model for a VSC

$$\frac{d}{dt} \begin{bmatrix} id \\ iq \end{bmatrix} = \begin{bmatrix} \frac{R}{L} & 0 \\ 0 & -\frac{R}{L} \end{bmatrix} \begin{bmatrix} id \\ iq \end{bmatrix} + \begin{bmatrix} x1 + \omega \cdot iq \\ x2 - \omega \cdot id \end{bmatrix} \quad (\text{EQ 4.16})$$

Thus we see that If we have  $u1=x1+\omega.iq$  and  $u2=x2-\omega.id$  as control variables, we get a complete decoupled response for the system. This suggests the control system of Fig 4.14, in which the PI regulator blocks control the variables  $u1$  and  $u2$ . The variable  $ed$  and  $eq$  which are actual injected voltages can be obtained as:

$$u1 - \omega \times iq = x1 = \frac{Vd - ed}{L} \quad (\text{EQ 4.17})$$

$$u2 + \omega \times id = x2 = \frac{eq}{L} \quad (\text{EQ 4.18})$$

Thus

$$ed = Vd - L \times (u1 - \omega \times iq) \quad (\text{EQ 4.19})$$

$$eq = -L \times (u2 - \omega \times id) \quad (\text{EQ 4.20})$$

A control system based on above model which decouples the real power P and reactive power Q control loops is shown below in Fig. 4.14. Note that the controller inputs are  $id$  and  $iq$  instead of  $p$  and  $q$ . However, it should be realized that instantaneous real power  $P=vd*id$  and instantaneous reactive power  $Q=vd*iq$ , so the  $id$  and  $iq$  orders are similar to the P and Q orders respectively. The PI controllers are coupled to each other in such a way that their net effect is to give a decoupled response. Note that as the SPFC element is inserted in the series with the line, the system voltage  $V$  is actually  $Vs-Vr$ , the difference between sending and receiving end voltages. If the actual value of  $Vr$  is used, then it must be communicated from the receiving end. Alternatively, it can be calculated only from the sending end quantities if we know of the transmission line impedance. It should be realized that in deriving the control block shown below, it was assumed that the measurements

of  $i_d$  and  $i_q$  from the system were instantaneous. In reality, there could be delay in these measurements due to instrumentation and filtering. If necessary, these additional delays can also be compensated for by introducing additional coupling in the PI control loops.

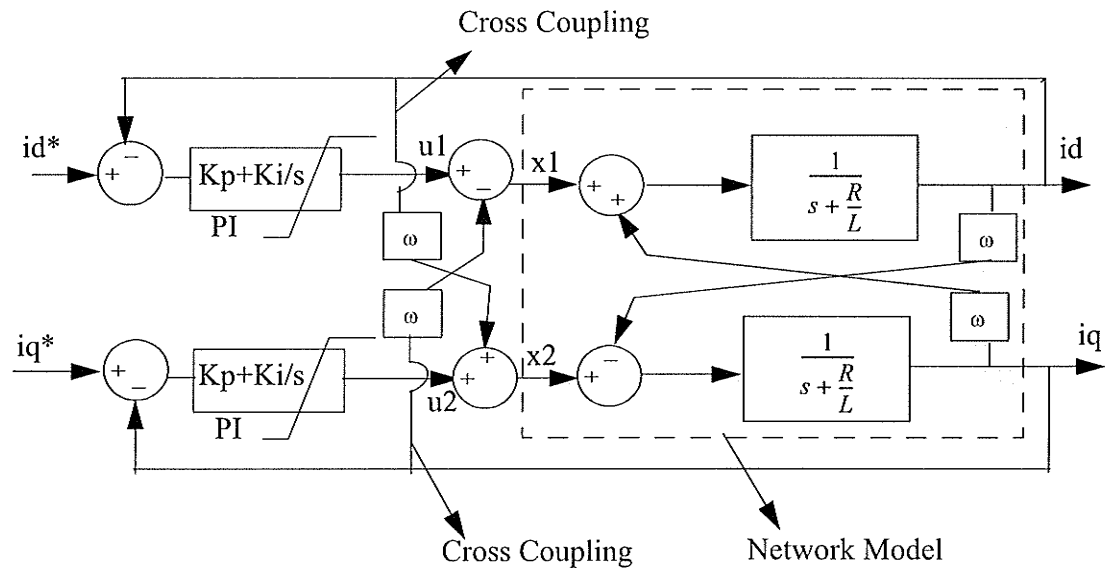


Fig. 4. 14 Decoupled d-q Control loops of a Converter Connected to the System.

#### 4.4 Overall Control System for the Complete UPFC

UPFC has many degrees of freedom and can be controlled in many ways. Both the shunt and series parts can be controlled using the decoupled technique discussed. The shunt part is usually controlled so that the DC bus capacitor is kept charged to its rated voltage. The reactive power order to the shunt controller could set to either zero or the output of a voltage regulator block that controls the AC bus voltage. The series element is the critical element as it allows for the control of the power flow in the line.

The shunt and series controllers from UPFC example case modelled in PSCAD/EMTDC will be discussed in the next chapter.

## CHAPTER 5      MODELING OF UPFC USING PASCAD/EMTDC.

---

### 5.1 Introduction

In Chapter four, we developed the mathematical model of UPFC for the point to point AC transmission network. We also derived control blocks for an open loop, coupled and decoupled d-q axis controller.

This chapter will discuss the development of a transient model which can be used to verify UPFC operation as well as for network application studies in the future. Hence the objective of this chapter is to build a UPFC model on PSCAD/EMTDC simulation software to determine the steady state capabilities of UPFC, and then apply learnt control methods from chapter four to control independently AC transmission network's real and reactive power. This part of research will also analyse the accuracy of derived open loop and decoupled d-q axis control methods against the simulation results.

As mentioned before, UPFC is a combination of Shunt Converter and Series Converter which are coupled via a common DC link (Capacitor). As the series converter of UPFC is the principal operational component (the shunt being used primarily for DC power supply). We initially develop the model for the series part of UPFC. SSSC is controlled using SPWM [14], [Appendix B] as also discussed earlier in chapter 4 section 3. Also for the purpose of the control design, we first represent the converter itself as a controllable Sinusoidal AC voltage. We will later replace this with a full converter model.

## 5.2 Modeling of a Series Converter

To simplify SSSC model, we assumed that the DC circuit consists of a strong DC voltage source with the ability to carry out real power exchange with the AC system. Note that the shunt converter eventually maintains this DC supply.

We review following parameters before building SSSC model on PSCAD

- Line parameters of a given AC transmission network.
- Transmittable power ratings of the AC transmission network.
- Transmission network voltage.
- Magnitude of the injected voltage in series with the transmission network.

For the simulation purpose, we considered the application of UPFC on a 230 KV AC long transmission line. The impedance for such a line is assumed to be  $X_L=500$  ohms which with a typical power transmission phase angle ( $\delta$ ) of 30 degree results in a real and reac-

tive power measurement of 53 MW and -14 MVAR, respectively. The real power transmission level of 53 MW is too small in comparison with the shorter 230 KV lines and it needs to be increased with same set of series compensation.

The simulation model of SSSC is shown in the Fig. 5.1.

In this initial model, SSSC is represented by the sinusoidal voltage source Dva, Dvb and Dvc with variable magnitude and phase angle.

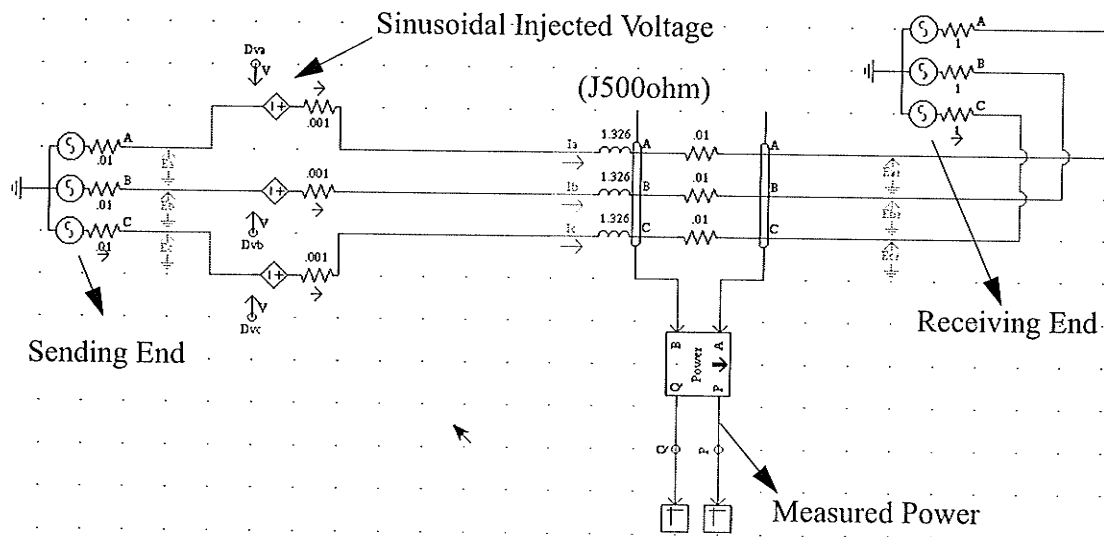


Fig. 5. 1 Modeling of Series Branch of UPFC

The open loop d-q component control block is modelled as shown in Fig 5.2 which is the PSCAD/EMTDC representation for Fig (4.11b). The open loop controller controls independently transmission line's real and reactive power within a specified limit given by the magnitude of the injected voltage.

As shown in the Fig 5.2, this control method calculates the magnitude and phase angle of the injected voltage of each phase in series with the transmission network from a

demanded real power  $P^*$  and reactive power  $Q^*$  by multiplying the desired increments  $\Delta P$ ,  $\Delta Q$  of the real and reactive power by  $\cos(\omega t)$  and  $\sin(\omega t)$ , respectively. The signal  $\cos(\omega t)$  or  $\sin(\omega t)$  can be obtained from a PLL which tracks the voltage of the sending end busbar.

Here the AC transmission line is considered to be a pure reactance with no losses.

$$\Delta P = \text{order real power } (P^*) - \text{measured real power } (P_o)$$

$$\Delta Q = \text{order reactive power } (Q^*) - \text{measured reactive power } (Q_o).$$

Any transient ripple in the measured power is removed by filtering through a Fast Fourier Transform (FFT) based on digital filter.

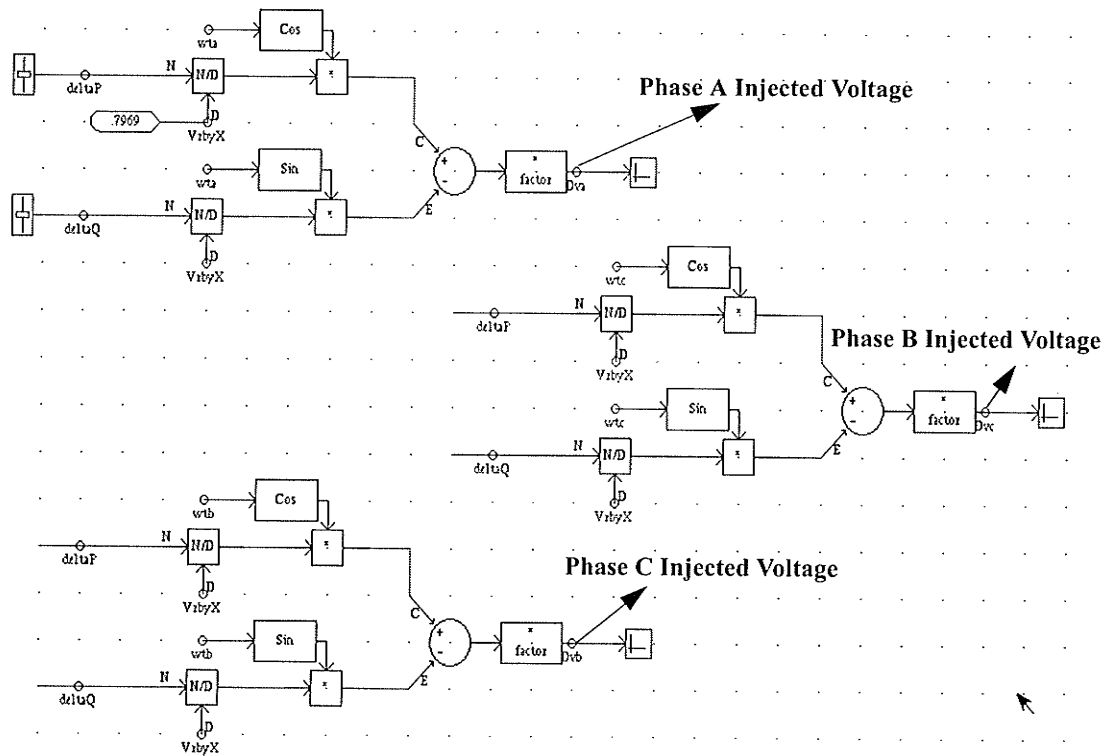


**Fig. 5. 2** An Open Loop d-q Component Controller of the Series Branch of UPFC

Fig 5.3 shows the simulation results. The system is started with the SSSC turned off (zero injection stage) which results in the uncompensated line power flow of 53 MW, -14 MVAR, consequently several changes of 10 or 20 MW are sequential applied to the real power order in the first 5 second of the simulation. The system is again returned to zero injection state at 5 second, and similar changes are made to the reactive power order in the next 5-10 second interval. The results of Fig 5.3 show that although the changes in real power  $P^*$  do not result in changes in reactive power  $Q^*$  in the steady state, they do result in transient state.

For example, a step change of 10 MW in the real power introduces a 15% transient disturbance in the reactive power of the network and vice-versa (see Fig 5.3).

The steady state response of these control loops are in agreement with the derived equations in chapter three.

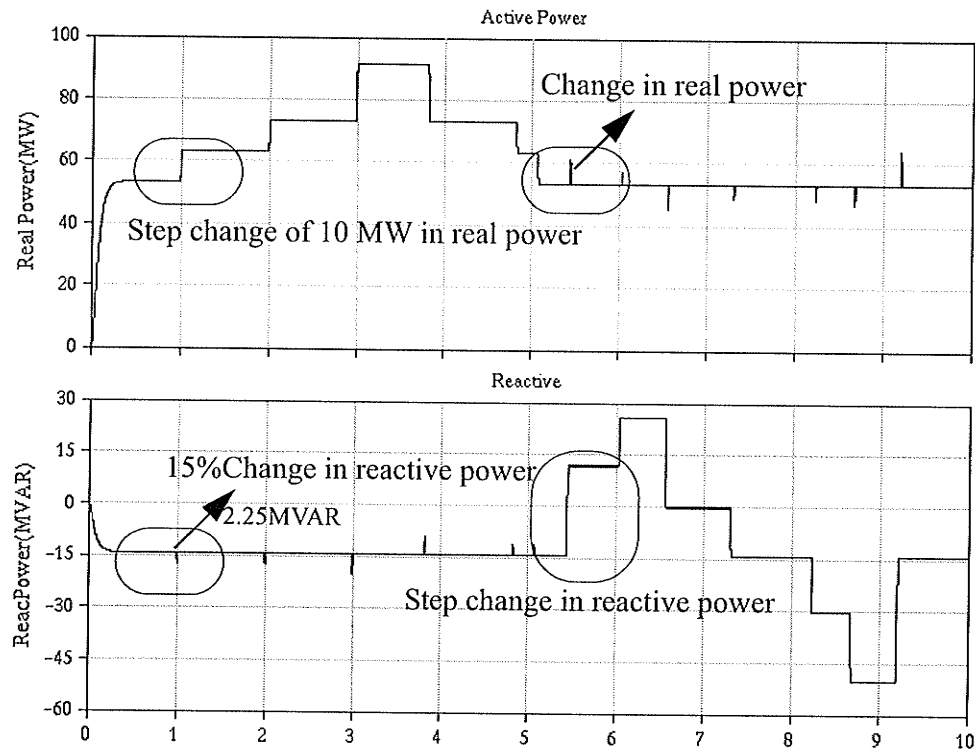


Fig. 5.3 Open Loop d-q Component Control method of a Series Converter

Nevertheless, these control methods offer simplified understanding of SSSC control.

### 5.2.1 PWM based d-q controller for the Series Converter of UPFC

In the previous section, we used an idealized representation of the series converter (controlled sinusoidal AC source) in order to evaluate the basic control strategy. Here a more detailed representation which includes the semiconductor switching of the converter to gain required injected series voltage is utilized. The shunt converter is still not modelled and its effect is included with the DC side voltage source of 20 KV.

As seen from Fig 5.4, PWM based converter converts a DC voltage into a three-phase output voltage through a coupling transformer. These injected voltages  $E_{ss1a}$ ,  $E_{ss1b}$  and  $E_{ss1c}$  for a order real power ( $P^*$ ) and reactive power ( $Q^*$ ) are in series with the transmission line. Their order values  $D_{va1}$ ,  $D_{vb1}$  and  $D_{vc1}$  are calculated by the designed control scheme (see Fig 5.2). PWM controller converts these voltage orders to firing signals for IGBT semiconductor as shown in Fig 5.5 in the manner discussed in Appendix A.

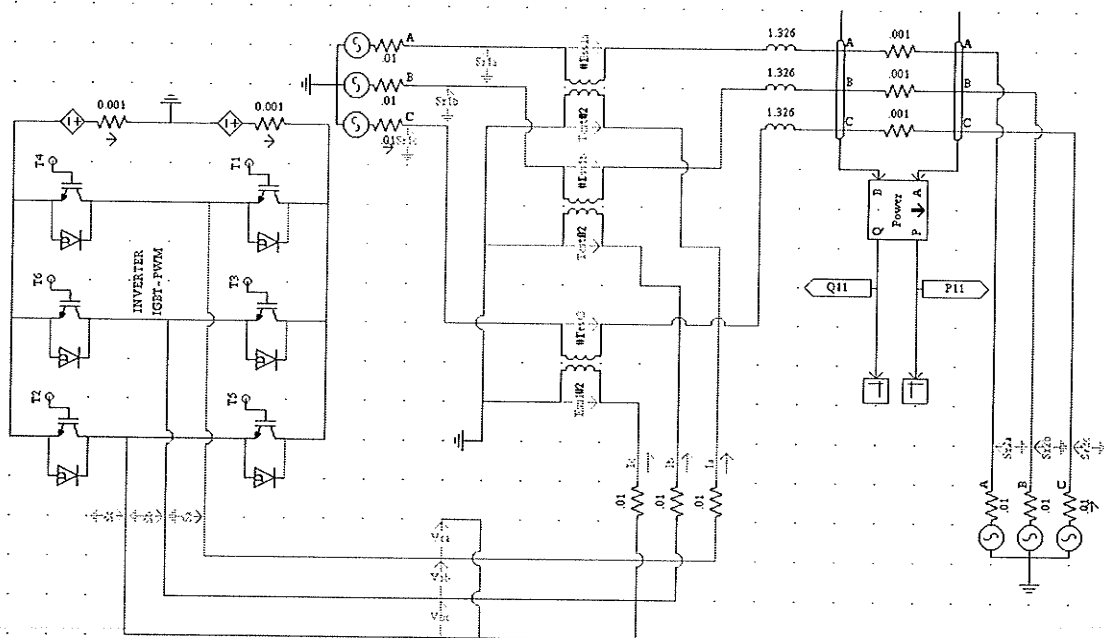


Fig. 5. 4 PWM based Series Converter

The output signals from PWM are PLL with the terminal sending end voltage.

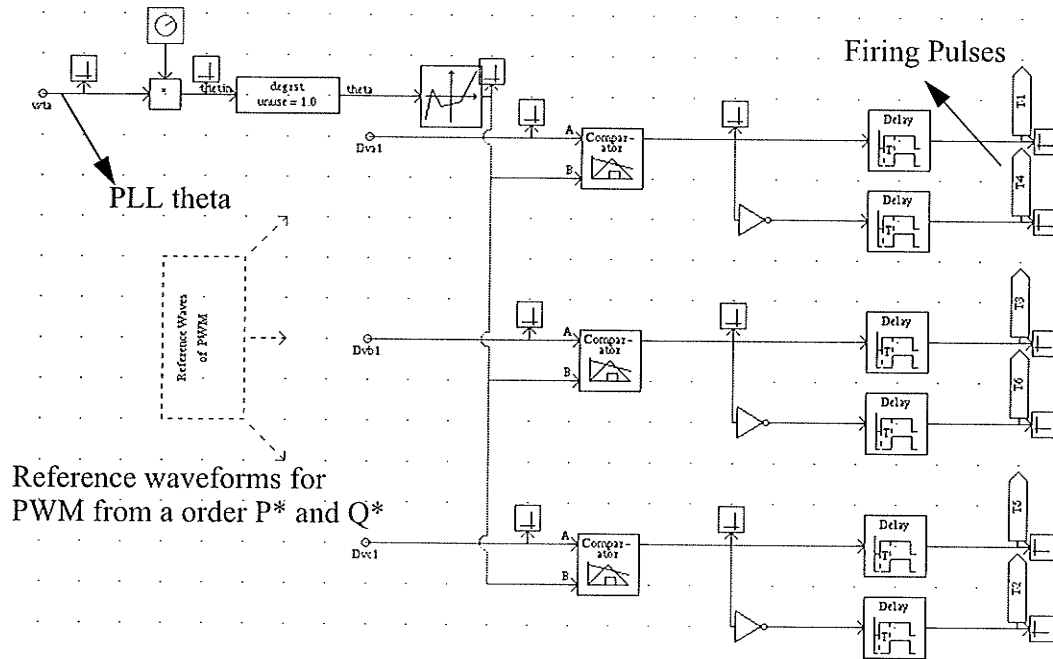


Fig. 5.5 Firing Pulses of PWM for Series Converter

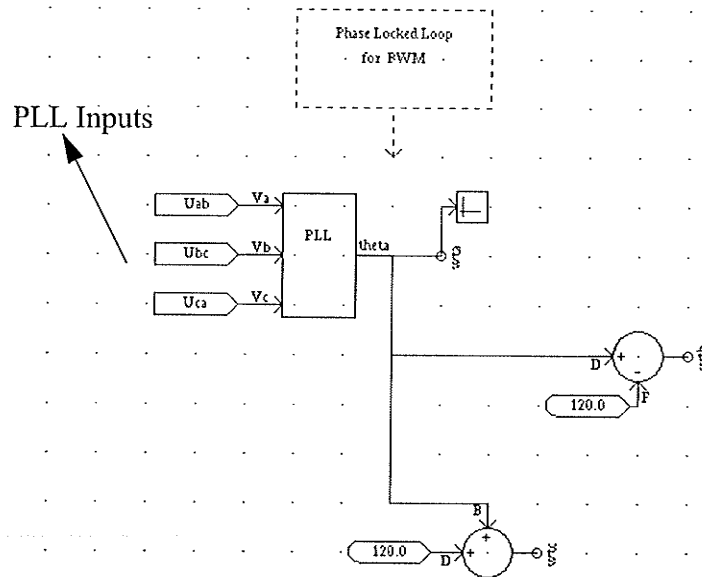


Fig. 5.6 Phase Locked Loop of Series Converter

The simulation results shown in the Fig 5.7 confirms that a step change of 10 MW in the real power does introduce a transient disturbance in the reactive power of the network, and vice-versa.

The performance is similar to that of the idealized source. This shows that even the idealized representation is acceptable for most studies.

Open Loop Control of PWM based Series Converter of UPFC

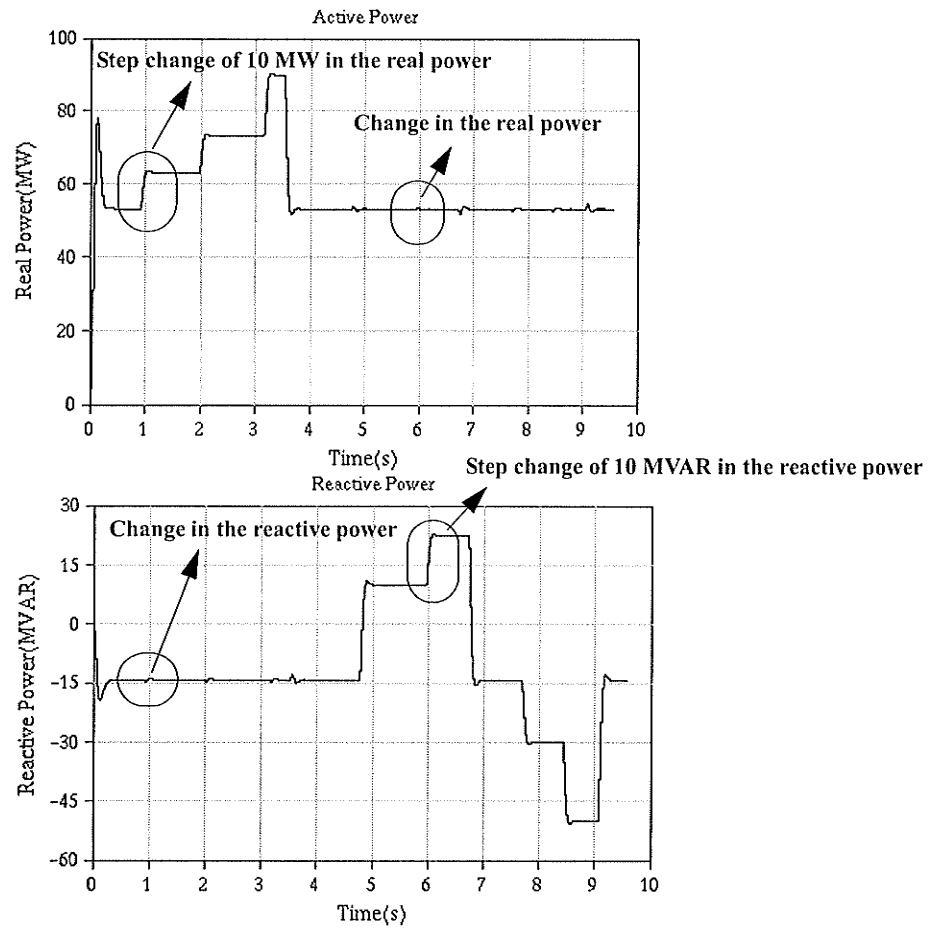


Fig. 5. 7 PWM based d-q Component control method of a Series Converter.

### 5.2.2 Decoupled d-q axis controller for the Series Converter of UPFC

In order to improve the performance of UPFC and reduce the interaction between its real and reactive power control loops during a transient state, a so-called decoupled watt-var control algorithm discussed in chapter four (section 3, (Fig 4.14) has been implemented to build a Series Converter.

Here the transmission line connected to a length of 100km, and the smaller X and R values are used as they accentuate the coupling between the controllers. Hence If the decoupled system works well with the shorter line, This system will also work with the longer line.

The simplified equivalent 230 KV AC transmission network of a series connected voltage source converter with the transmission line resistance 5.29 ohms and impedance 52.9 ohms ( $R/X=.1$ ) is shown in Fig 5.8. For  $\delta = 20^\circ$ , the steady state transmitted real and reactive power capabilities are 341 MW and 25 MVAR, respectively.

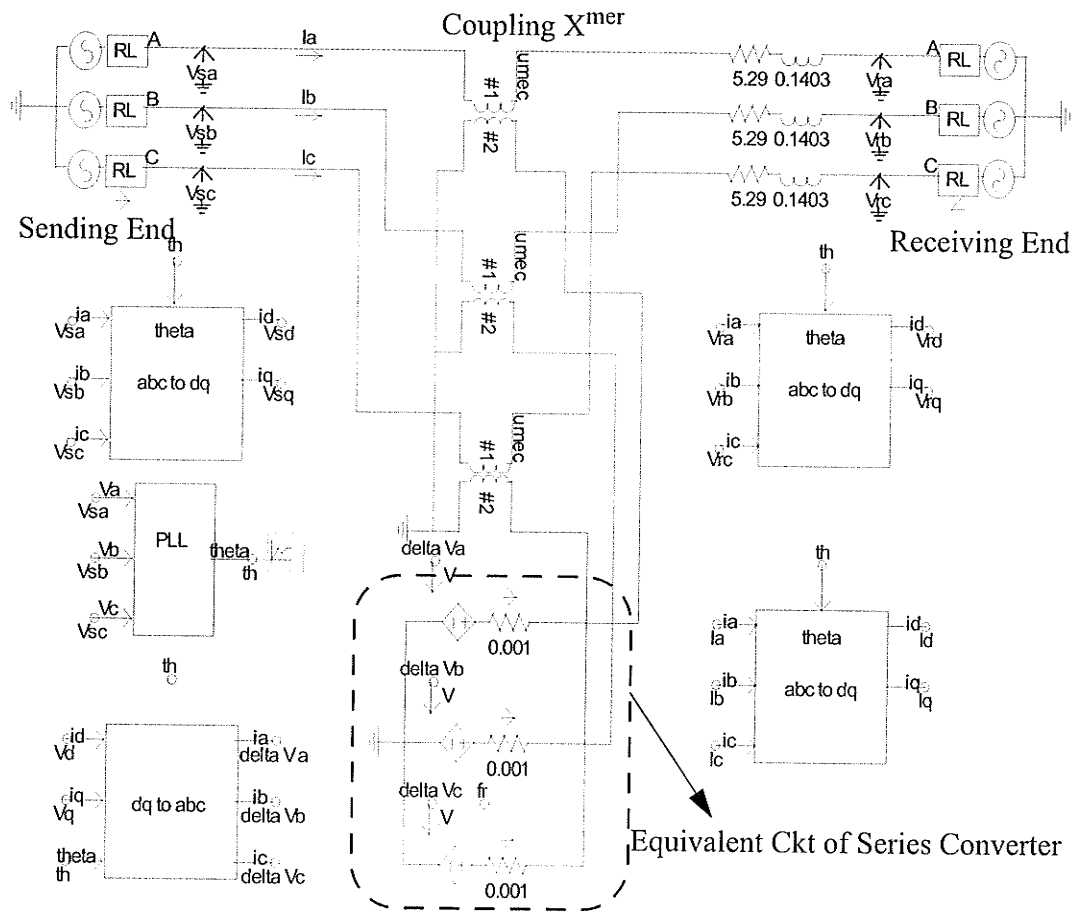


**Fig. 5. 8** Simplified Equivalent AC transmission Network of a Series Connected Voltage Source Converter.

As shown in Fig 5.8, the input values for decoupled d-q axis controller are as follows;

- Instantaneous values of sending and receiving end voltages;  $V_{sa}$ ,  $V_{sb}$ ,  $V_{sc}$  and  $V_{ra}$ ,  $V_{rb}$ ,  $V_{rc}$ .
- Line currents  $I_a$ ,  $I_b$  and  $I_c$ .
- Order  $I_d^*$  and  $I_q^*$ .

By using three phase to d-q vector transformation [Appendix B], the transformation of balanced three phase variables to instantaneous vectors can be applied to the AC analog values (voltage and current) on both the sides of the AC network. A new coordinate sys-

tem [22] is defined where d axis is always coincident with the instantaneous sending end voltage vector  $V_{sd}$ . Here the d-axis component of the sending end voltage vector is represented by  $V_{sd}$  and the q-axis component  $V_{sq}$  (conceptually equal to zero).

Note that In power system, it is customary to develop the controller in terms of a normalized, or per unit (pu) representation. This permits the same developed controller to be used on equivalent system of different voltage and current ratings. The method of obtaining these is discuss below.

The transformed three phase voltages and currents into d-q axis can also be used to derive instantaneous power in terms of d-q quantities by

$$P(t) = \frac{3}{2}(V_{sd} \cdot I_d + V_{sq} \cdot I_q) \quad (\text{EQ 5.1})$$

$$Q(t) = \frac{3}{2}(V_{sq} \cdot I_d - V_{sd} \cdot I_q) \quad (\text{EQ 5.2})$$

Under balanced conditions, the coordinates of the voltages and current vectors in the synchronous reference frame (described above) are constant quantities.

Considering that the q component of the sending end voltage is equal to zero, the real and reactive power given by equations (5.1) and (5.2) can be simplified in per unit system which are as follows:

$$P_s = V_{sd} \cdot I_d \quad (\text{EQ 5.3})$$

$$Q_s = V_{sd} \cdot I_q \quad (\text{EQ 5.4})$$

From equations (5.3) and (5.4), we could derive d - q axis currents in per unit as shown in Fig 5.9. Here the base VA is 100 and Voltage is 187.79 KV (peak phase voltage).

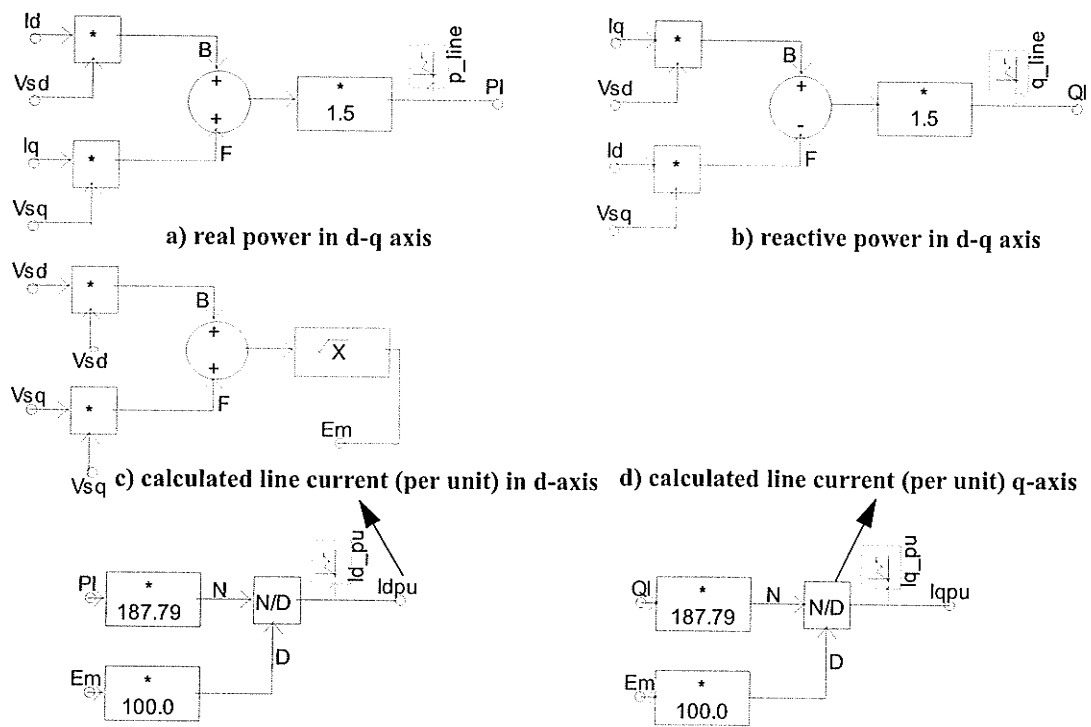


**Fig. 5.9** d-q Vector Transformation of Instantaneous Three Phase Quantities.

These per unit values (as shown by the Fig 5.9) of derived currents,  $I_{d_{pu}}$  and  $I_{q_{pu}}$ , are compared with per unit reference values of current,  $I_{d\_ref}$  and  $I_{q\_ref}$ , respectively in the control system described in Fig.5.10 (redrawn from Fig 4.14)

From equations (5.3) and (5.4), the reference real and reactive power at the sending end are equivalent to  $I_{d\_ref}$  and  $I_{q\_ref}$ , respectively

The resulting current error signal is fed to the Proportional Integrator (PI) Controller which in turn provides the required converter output voltages  $V_d$  and  $V_q$  in such a way that reduces the current error signal is reduced to zero. As described in the chapter 4, Both

the d-q axis components of the line currents are cross-coupled through the term  $\omega$ . The PI controllers are coupled to each other in such a way that their net effect is to give a decoupled response. Decoupled d-q controller, as shown in Fig 5.10, is redrawn from Fig 4.14.

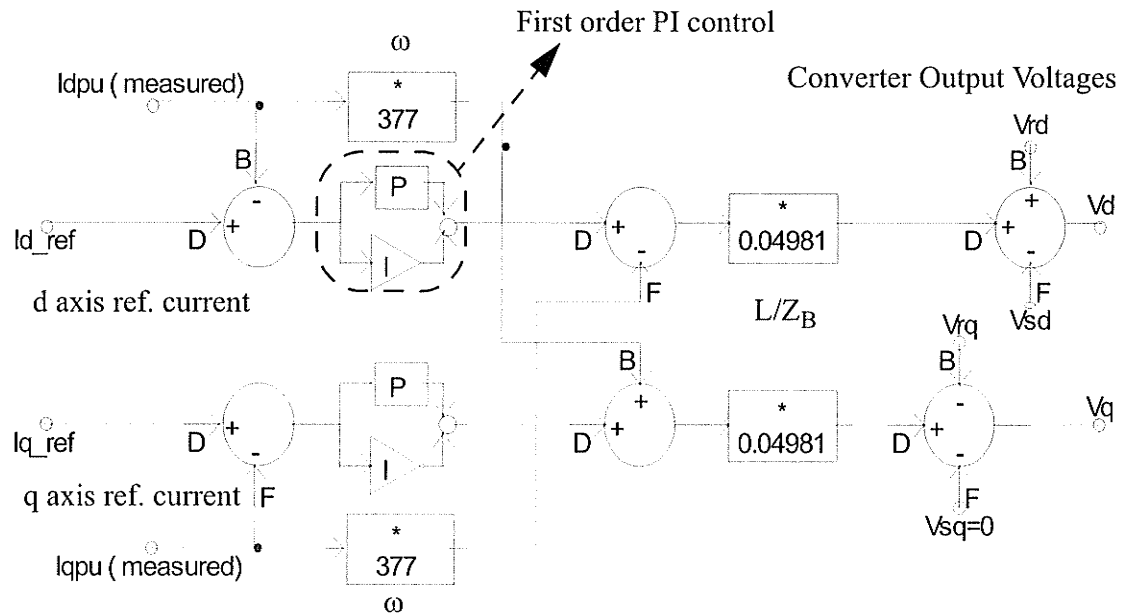


**Fig. 5. 10** Decoupled d-q Controller of the Series Converter

Here the proportional gain and integral time-constant of the first order PI controller were obtained by considering the minimum current overshoot of the system. The assumed value of the time constant should be 5ms or more (trial and error method).

Assuming the time constant  $T = 20$  ms.

the proportional gain  $K_p = 1/T = 50$

integral time-constant  $T_1 = .0005305$  sec.

System outputs were observed for the minimum current overshoot.

As shown in Fig 5.8, the converter output voltages ( $V_d$  and  $V_q$ ) are fed to a dq-abc converter block which has a PLL input ( $\theta$ ) tracking the voltage of the sending end busbar. The output of the dq-abc converter block provides an equivalent converter's output voltages ( $\Delta V_a$ ,  $\Delta V_b$  and  $\Delta V_c$ ) for the order real and reactive power flow in series with transmission line.

In this section, we used an idealized representation of the series converter (controlled sinusoidal AC source).

The simulation result of this controller is shown in Fig 5.11. It can be seen that the decoupled d-q axis controller offers improvement in terms of the response time for a order  $I_d$  (real power) and  $I_q$  (reactive power), respectively and also reduce the interaction between the real and reactive power control. Here the response time to reach 90% of the order real power is 3 fundamental frequency cycle (51ms).

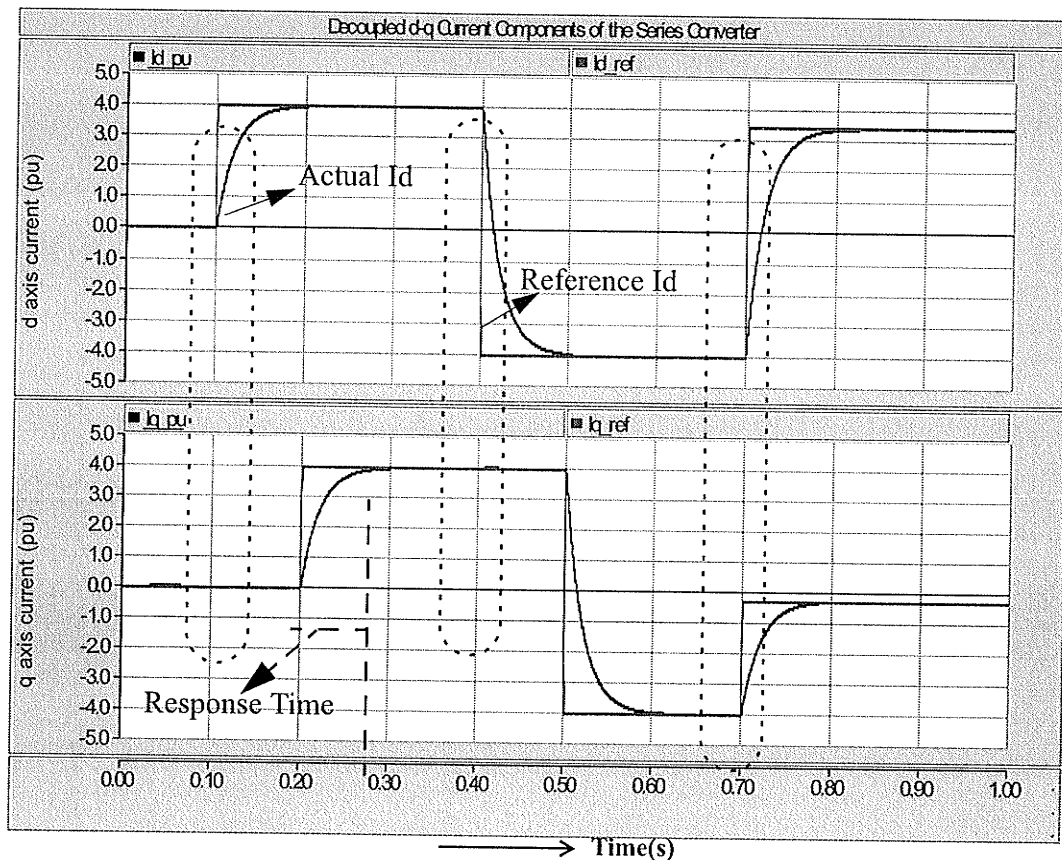


Fig. 5. 11 Performance of decoupled d-q Controller.

During the simulation, it was clearly observed that for a change of real power from 0 to 4 pu, there was no change in the reactive power of the Series Connected Voltage Source Converter. Similar to this, for a change of reactive power from 4 to 0 pu, there was no change in the system's real power.

This confirms the absence of interaction between d and q control loops.

### 5.3 Modeling of the full UPFC

In this part of the research we started with the series part of UPFC modeled as sinusoidal voltage source. Then we introduce PWM based series converter in the AC network which includes the modeling of semiconductor switching, but we still represented the effect of the DC converter as a constant voltage source. Once we succeed in this representation, we moved to the next step of the research by removing the constant approximation and then properly representing the shunt converter which provides the DC side supply for the series part.

The block of full UPFC as shown in Fig 5.12 has the decoupled d-q controller implemented on both the shunt and the series parts of UPFC. Note that the reactive power order to the shunt controller is set to zero.

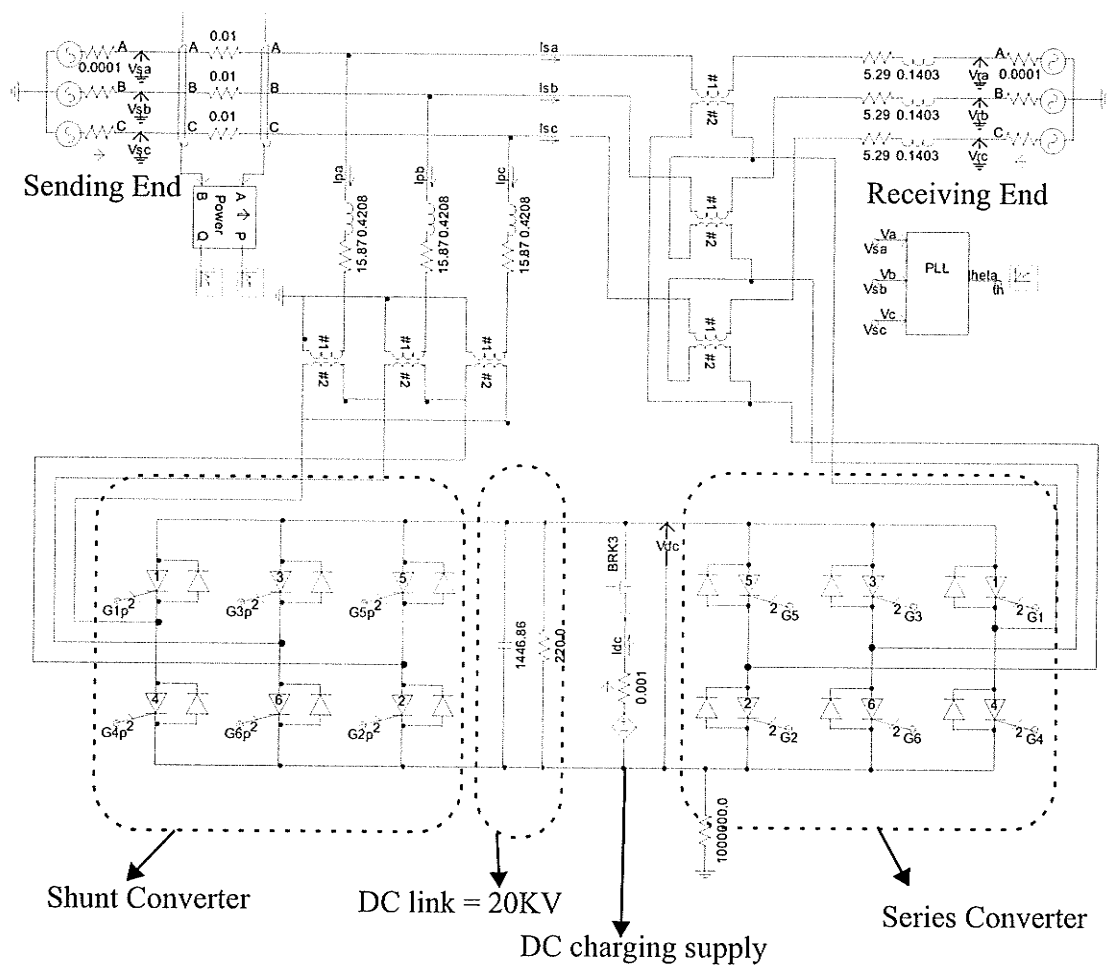


Fig. 5. 12 Decoupled d-q Controller Based UPFC

**Series Part Simulation Result**

As discussed in chapter four, we decided (due to the cost constraint of the devices) to inject  $\Delta V_{\text{maximum}} = .5$  pu of the system voltage in series with the transmission line. The range of  $\Delta V$  injected voltage by the shunt converter in this model is as follows:

$$0 \leq \Delta V \leq 93.87KV$$

The simulation results of PWM based UPFC for the independent control real and reactive power flows is shown in Fig. 5.13

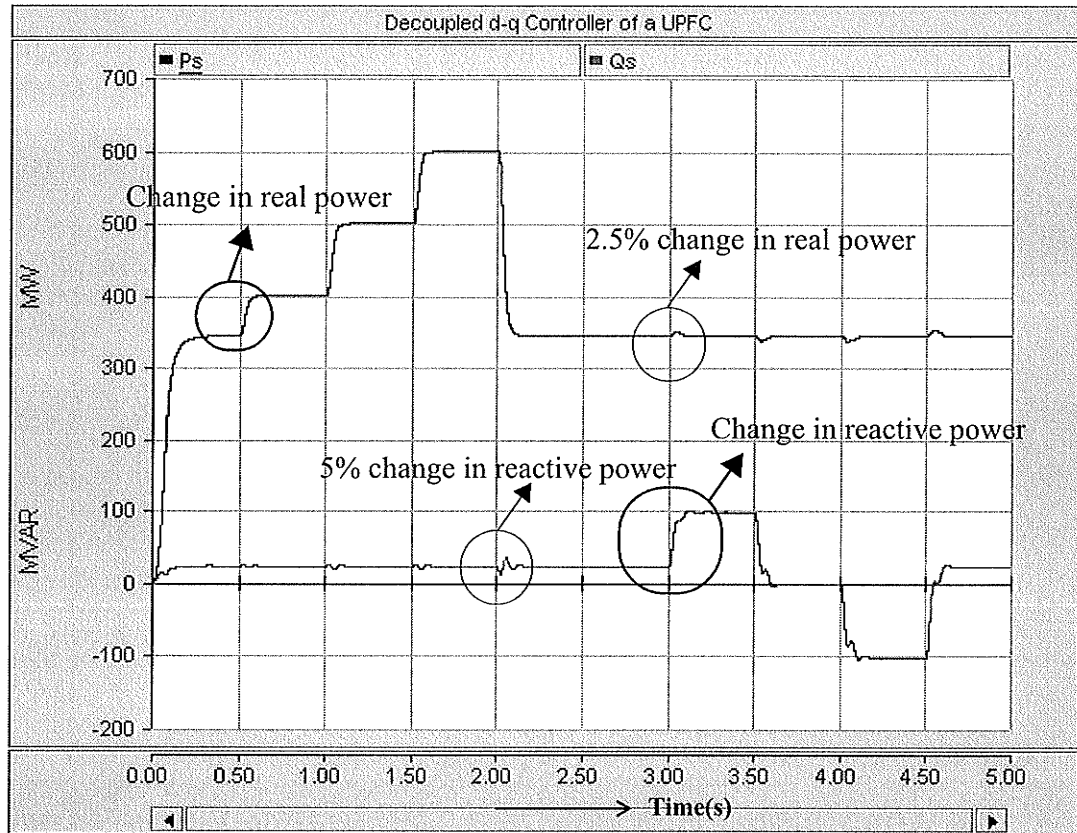


Fig. 5.13 Independent control of real and reactive power by UPFC

The simulation results shown in the Fig 5.14 confirms that the q component of the series injected voltage affects only the real power flow and the d component the imaginary power.

Here a change of 0.1627 pu (from zero voltage injection state) in the order real power enforces the respective changes of 0.06 pu in the q component of the series injected voltage  $V_q$  and visa- versa. This decoupling error is because of ripple on DC bus voltage

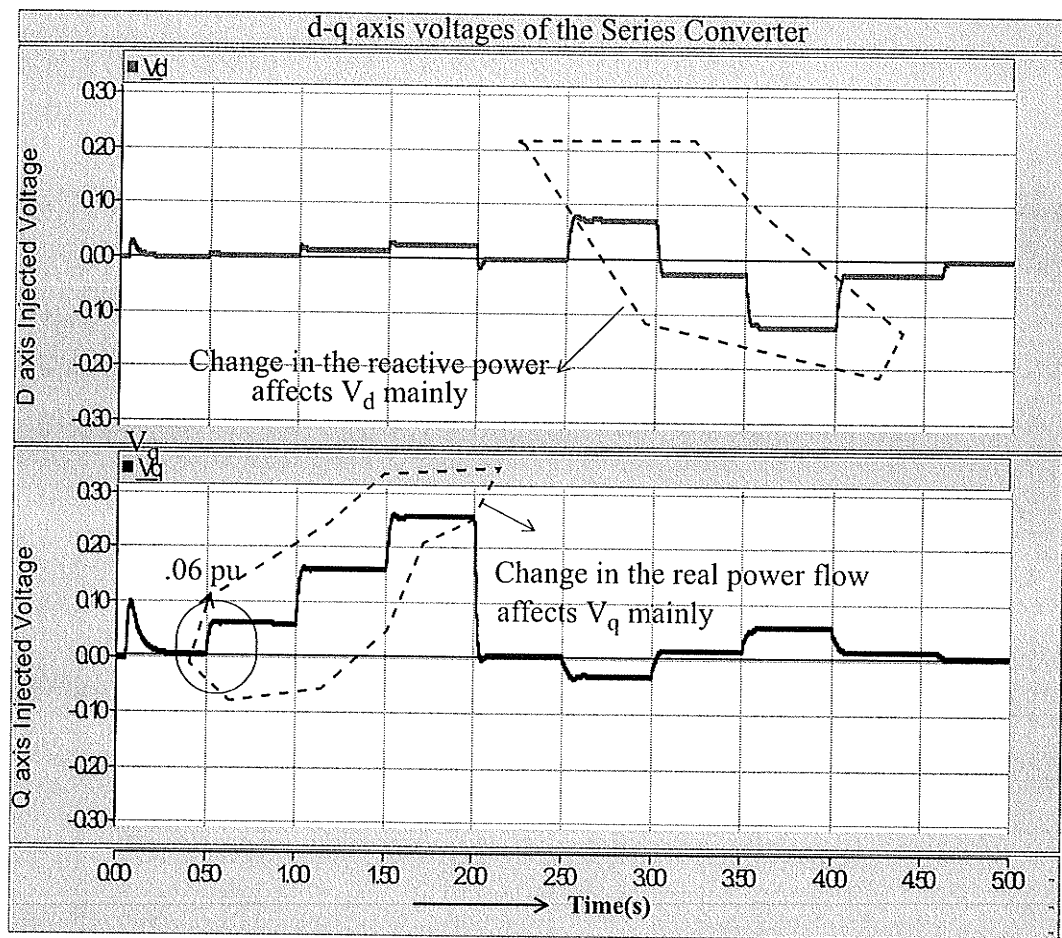


Fig. 5. 14 Series Converter's d-q axis Output Voltages  $V_d$  and  $V_q$ .

### Capacitor Voltage

A DC charging supply is shown in Fig 5.12. This supply charges the DC capacitor at start-up and then the supply is switched off. This charging supply may not be present in the real system; but is used to quickly start-up the system, so that we do not have to consume computer time to simulate the start up process.

The shunt converter is designed to regulate the DC bus voltage; however a sudden demand for the power by the series converter still causes a transient in the DC voltage. This is seen in Fig 5.15, where the capacitor voltage (DC link) changes from + 12% for the above changes in the real and reactive power of the AC transmission line respectively.

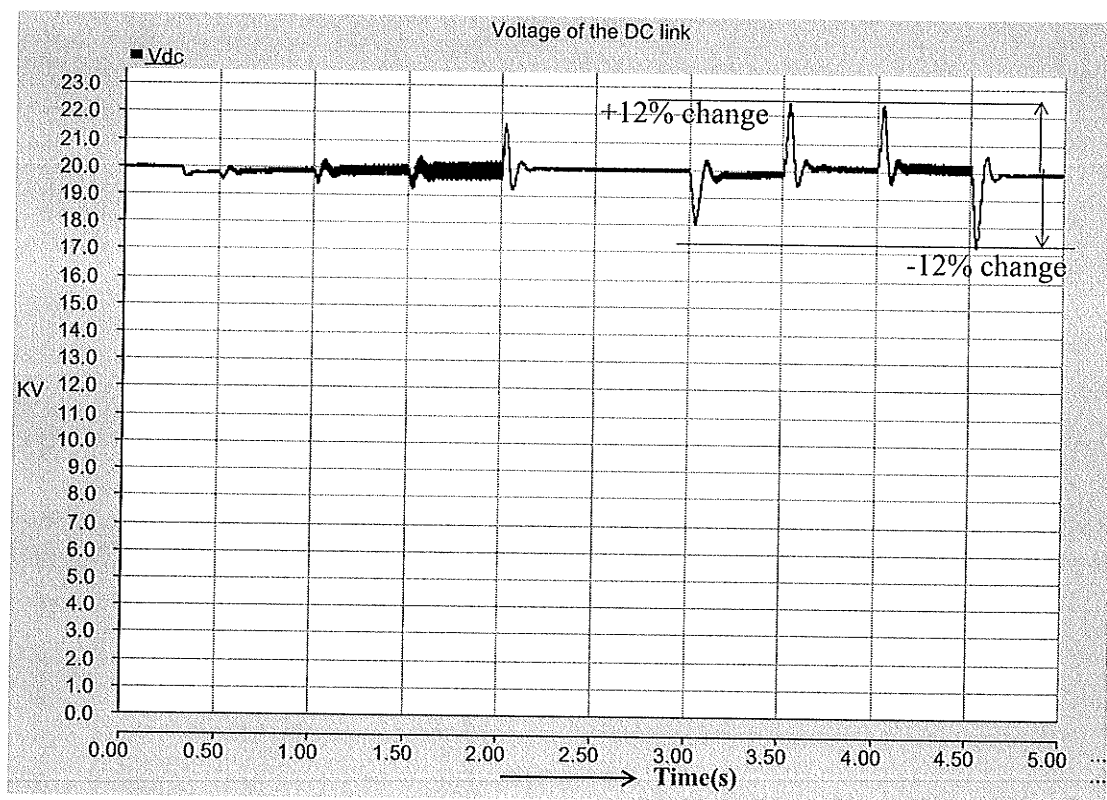


Fig. 5.15 Capacitor Voltage of UPFC

This 12% variation could be reduced by increasing the size of the capacitor.

**Shunt Converter Control**

The d-q axis real and reactive power of the shunt branch is shown in the Fig. 5.16. Considering that the q component of the sending end voltage  $V_{sq}$  is equal to zero, the shunt real power and reactive power can be simplified in the following equations:

$$P_{Shunt} = V_{sd} \cdot I_{pd} \tag{EQ 5.5}$$

$$Q_{Shunt} = V_{sd} \cdot I_{pq} \tag{EQ 5.6}$$

From these equations and initial findings about series converter which says the q component of the series injected voltage affected the real power flow and the d component the imaginary power flow, we could conclude that any change in the orderd real power flow of the series part of UPFC will not make significant changes in the  $P_{Shunt}$ . However, any change in the order reactive power flow of the series part of UPFC will make significant changes in the  $P_{Shunt}$  (due to discharge of the capacitor voltage). The simulation result shown by Fig 5.17 also confirms the theoretical conclusion.

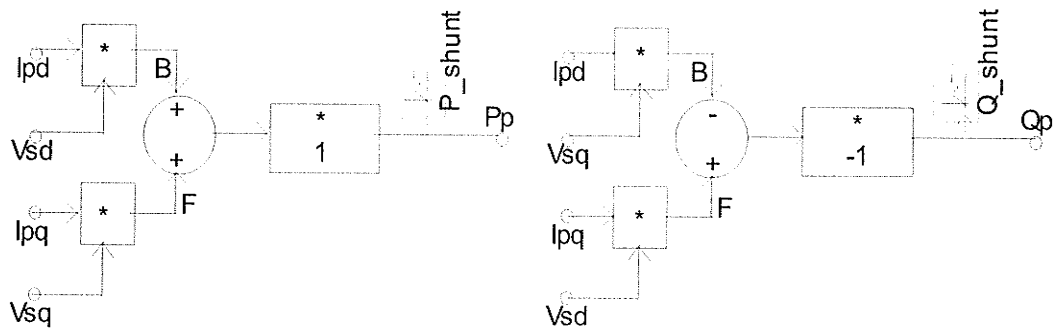


**Fig. 5. 16** Decoupled d-q Controller of the Shunt part of UPFC

### Shunt Part Simulation Result

The simulation results show the reactive power of the shunt part is kept close to the zero except a few transient periods.

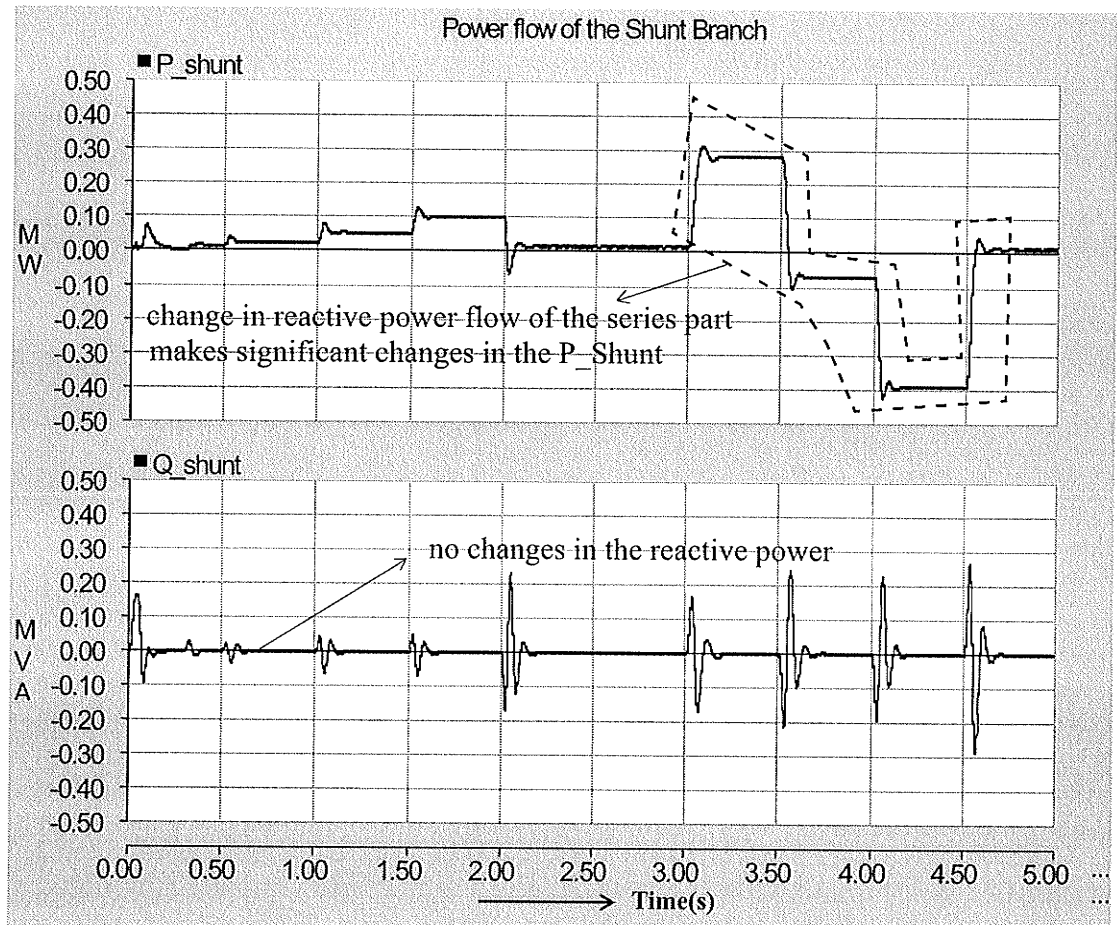


Fig. 5. 17 Response of the shunt part of UPFC

#### 5.4 Improvement for Control Implementation in Actual Network

UPFC has many degrees of freedom and can be controlled in many ways. Both the shunt and series parts of UPFC can be controlled using the decoupled d-q technique discussed in chapter four. The accuracy of the developed mathematical model in the chapter four was further successfully confirmed by the simulation results using PSCAD/EMTDC (see Fig 5.11). The results from the simulations confirm a close relationship with the derived mathematical model.

It is also realized that in deriving the control blocks in chapter four, it was assumed that the measurements of  $I_d$  and  $I_q$  from the system were instantaneous. In actual network, there could be delay in these measurements due to instrumentation and filtering. Considering this case, the current compensation for the above control blocks is not perfect, and therefore the system performance will be reduced.

If necessary, these additional delays can also be compensated for by introducing additional first order system block in an internal predictive control loop as discussed below

If we solve equation (4.16) as discussed in the chapter 4 for  $i_d$ , we would get a first order equation:

$$\frac{d}{dt}i_d + \frac{R}{L}i_d = u_1$$

By applying Laplace Transform here,  $i_d$  is

$$i_d = \frac{u_1}{s + \frac{R}{L}}$$

so a delayed  $u_1$  is a measure of  $i_d$ , the delay being  $L/R$ . We can make the delay as  $L/R +$  additional measurement delay.

As shown in the Fig 5.18, the modified decoupled d-q control method is designed with an internal predictive control loop.

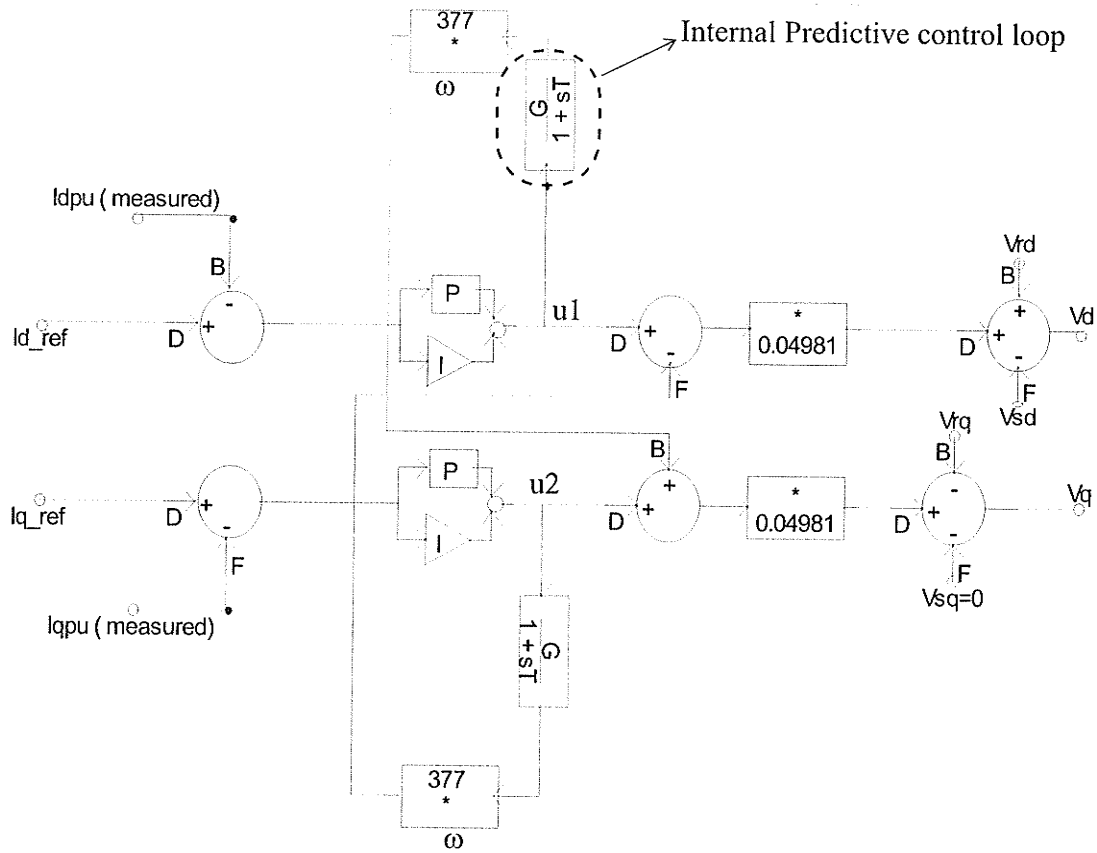


Fig. 5. 18 Modified decoupled d-q control method.

The above discussed modified decoupled d-q control method was implemented and PSCAD/EMTDC simulations were performed on the Series Converter model as shown in Fig 5.18. The steady state response of the modified decoupled d-q loop method was similar to the classical decoupled d-q control method (see Fig 5.19).

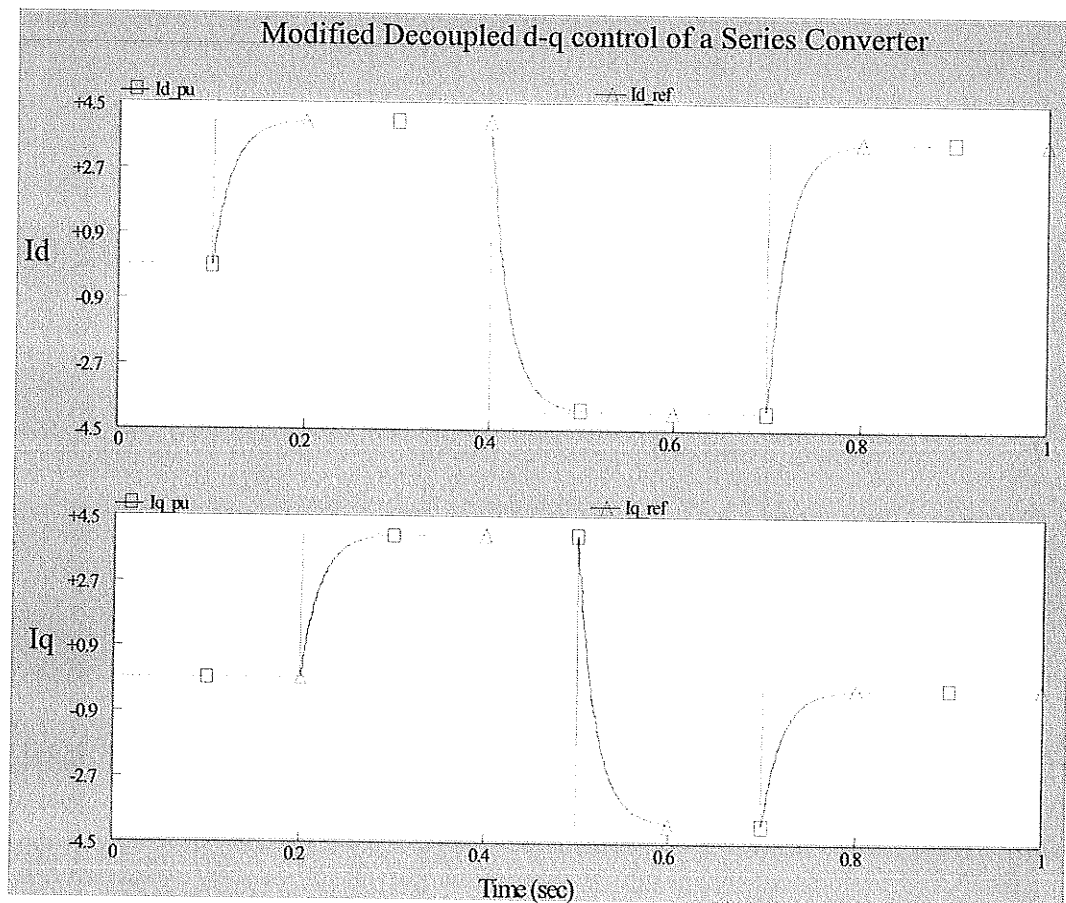


Fig. 5.19 Modified Decoupled d-q control of a Series Converter

## CHAPTER 6      Conclusions and Recommendations

---

### 6.1    Conclusions

The research objective was to understand the control methods of UPFC and its unique capabilities in independently controlling the real and reactive power flow for the AC transmission line and in allowing bidirectional flow of real power between the series converter output terminal and shunt converter output terminal.

The derivation of a mathematical Framework of UPFC and the understanding of its basic operating principles were discussed. This framework confirmed the superior capabilities of UPFC in power flow applications over the traditional reactive power compensators.

The mathematical framework was used to design various control systems such as Open Loop, Coupled and Decoupled d-q control blocks of UPFC, and to compare their performance in offering independent control of real and reactive power compensation.

In the AC transmission line with the resistance included, any transient change in the order line real power could affect the line reactive power, and vice-versa, without a proper compensation. Hence a so-called decoupled watt-var control algorithm [19] was used in improving the performance and in reducing the interaction between the real and reactive power control loops during a transient state.

Thus we introduced two control loops, each affecting only the d, or the q component of the injected series voltage at a time. The q component of the series injected voltage affected mainly the real power flow and the d component mainly the imaginary power flow. The injected series voltage signal was obtained from a phase-locked loop (PLL) which tracked the voltage of the sending end busbar.

Based on the derived decoupled control system, a transient model was designed for UPFC to use it for further studies.

The simulation results of UPFC (decoupled d-q techniques) showed a close relationship with the derived mathematical model and also confirmed the independent control of the real and reactive power flow of the AC transmission line.

The voltage source model was adequate for most controller studies.

## 6.2 Further Recommendations

This study is an interesting approach towards understanding the operation of a new device such as UPFC which is expected to be used frequently in supporting the real and reactive power demand in the power system grid. Recommendations for an extensive study on UPFC are enlisted below:

1) The performance of UPFC for controlling real and reactive power of the AC transmission line was studied assuming that the sending and receiving end voltages and transmission line phase angle were constant. This unique versatility of UPFC for controlling the power flow should be further studied under power system disturbances (such as power system oscillations).

UPFC performance needs to be measured under dynamic conditions such as AC transmission line faults and loop power flow, and then compared with the results of the conventional reactive power compensators.

2) UPFC simulation model should be modified to include harmonics filter which attenuates the harmonics generated by the inverter [25] and be checked for any effect from the filter dynamics.

3) UPFC simulation should be extended to understand the frequency response [26] of UPFC in a large power system network.

## APPENDIX A Sinusoidal Pulse width modulation

As shown in Fig A1, the switches in the voltage source inverter can be turned on and off as required. In the simplest approach, the top switch is turned on and off only once in each cycle, a square wave waveform results. However, if turned on several times in a cycle an improved harmonic profile may be achieved.

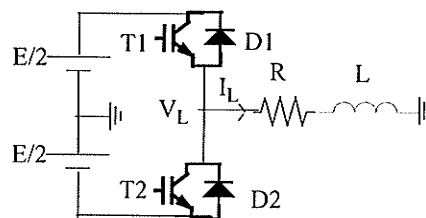


**Fig. A1** Simple Voltage Sourced Inverter

In the most straightforward implementation, generation of the desired output voltage is achieved by comparing the desired reference waveform (modulating signal) with a high-

frequency triangular 'carrier' wave as depicted schematically in the figure below. Depending on whether the signal voltage is larger or smaller than the carrier waveform, either the positive or negative DC bus voltage is applied at the output. Note that over the period of one triangle wave, the average voltage applied to the load is proportional to the amplitude of the signal (assumed constant) during this period. The resulting chopped square waveform contains a replica of the desired waveform in its low frequency components, with the higher frequency components being at frequencies of an close to the carrier frequency. Notice that the root mean square value of the ac voltage waveform is still equal to the DC bus voltage, and hence the total harmonic distortion is not affected by the PWM process. The harmonic components are merely shifted into the higher frequency range and are automatically filtered due to inductances in the ac system.

When the modulating signal is a sinusoid of amplitude  $A_m$ , and the amplitude of the triangular carrier is  $A_c$ , the ratio  $m=A_m/A_c$  is known as the modulation index. Note that controlling the modulation index therefor controls the amplitude of the applied output voltage. With a sufficiently high carrier frequency. The high frequency components do not propagate significantly in the ac network (or load) due the presence of the inductive elements. However, a higher carrier frequency does result in a larger number of switchings per cycle and hence in an increased power loss. Typically switching frequencies in the 2-15 kHz range are considered adequate for power systems applications. Also in three-phase systems it is advisable to use  $\frac{f_c}{f_m} = 3k, (k \in N)$  so that all three waveforms are symmetric.

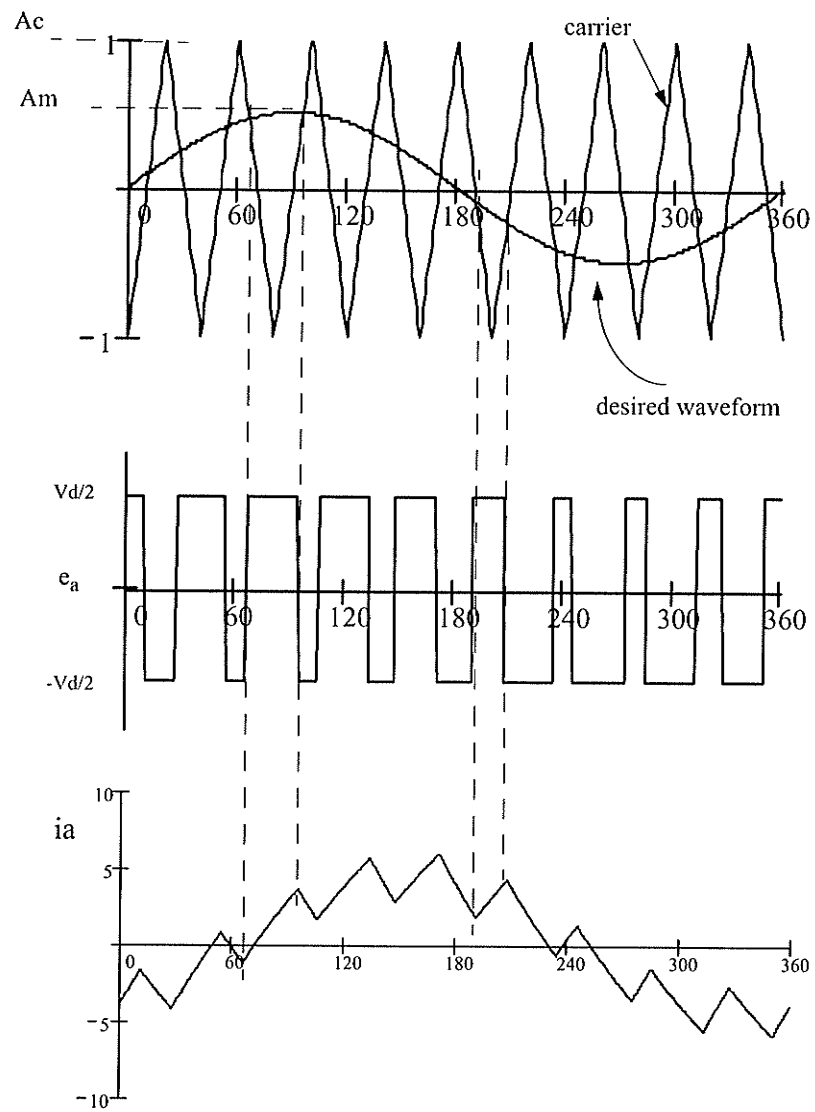


Fig. A 2 Principal of Pulse Width Modulation

## APPENDIX B     d-q transformation of three Phase Instantaneous Quantities.

---

### Introduction

The instantaneous real power at a point on the line is given by following equation

$$P = VaIa + VbIb + VcIc \quad 1$$

The above set of three instantaneous phase variables (such as  $V_a$ ,  $V_b$ , and  $V_c$ ), whose vector summation is zero, can be uniquely represented by a single point on a plan as shown in Fig A.1. By definition the vector drawn from the origin to this point has a vertical projection onto each of the three symmetrical disposed phase axis which corresponds to the instantaneous value of the associated phase variable. The transformation of the phase variables to instantaneous vectors can be applied to voltages ( $V_a$ ,  $V_b$  and  $V_c$ ) as well as to currents ( $I_a$ ,  $I_b$  and  $I_c$ ). As the values of the phase variables change, the associated vector moves around the plane describing various trajectories. The vector contains all the information on the three phase set including steady state unbalance, harmonic waveform distortion and transient components.

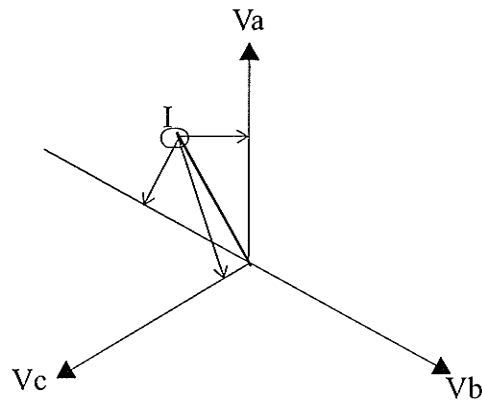


**Fig. A.1** Vector Representation of Instantaneous Three Phase Variables.

In the Fig A.2, the vector representation is extended by introducing an orthogonal co-ordinate system in which each vector is described by means of its d-q components. The transformation of the phase variables to d-q components are as follows

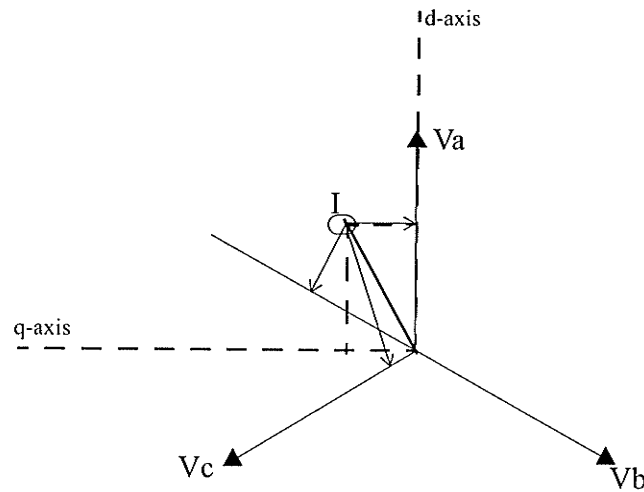


Fig. A.2 d-q components representations.

If  $V_a$ ,  $V_b$  and  $V_c$  are balance set of voltages,

$$V_a = \sqrt{2} \cdot V_{rms} \cdot \sin \omega t$$

$$V_b = \sqrt{2} \cdot V_{rms} \cdot \sin(\omega t - 120)$$

$$V_c = \sqrt{2} \cdot V_{rms} \cdot \sin(\omega t - 240)$$

So the d-q components for these three phase instantaneous quantities are as follows

$$\begin{bmatrix} V_d \\ V_q \\ i_0 \end{bmatrix} = \frac{2}{3} \begin{bmatrix} \cos(\theta) & \cos\left(\theta - \frac{2}{3}\pi\right) & \cos\left(\theta + \frac{2}{3}\pi\right) \\ \sin(\theta) & \sin\left(\theta - \frac{2}{3}\pi\right) & \sin\left(\theta + \frac{2}{3}\pi\right) \\ \frac{1}{2} & \frac{1}{2} & \frac{1}{2} \end{bmatrix} \begin{bmatrix} V_a \\ V_b \\ V_c \end{bmatrix}$$

Similar to this, three phase instantaneous currents can also be represented by d-q axis which are as follows

$$\begin{bmatrix} I_d \\ I_q \\ i_0 \end{bmatrix} = \frac{2}{3} \begin{bmatrix} \cos(\theta) & \cos\left(\theta - \frac{2}{3}\pi\right) & \cos\left(\theta + \frac{2}{3}\pi\right) \\ \sin(\theta) & \sin\left(\theta - \frac{2}{3}\pi\right) & \sin\left(\theta + \frac{2}{3}\pi\right) \\ \frac{1}{2} & \frac{1}{2} & \frac{1}{2} \end{bmatrix} \begin{bmatrix} I_a \\ I_b \\ I_c \end{bmatrix}$$

These vector representations lead to a definition of the instantaneous reactive current. Only the component of the current vector which is in phase with the instantaneous voltage vector contributes to the instantaneous power. The remaining component could be removed without changing the power, and that component is therefore the instantaneous reactive current.

These findings can be extended to define the instantaneous power in terms of d-q components which are as follows

$$P = \frac{3}{2}(V_d \cdot I_d + V_q \cdot I_q)$$

$$Q = \frac{3}{2}(V_d \cdot I_q - V_q \cdot I_d)$$

# References

---

## References

- [1] T.J.E Miller, "Reactive Power Control in Electrical Systems", John Wiley and Sons, NY 1982.
- [2] Mathur R.M. (Ed) "Static Compensators for Reactive Power Control", Canadian Electric Association, 1984.
- [3] Narain G. Hingorani; Laszlo Gyugyi "Concepts and Technology of Flexible AC Transmission Systems", 2001.
- [4] Phase shifting transformers in an efficient power flow control method.  
Papazoglou, T.M.; Popovic, D.P.; Mijailovic, S.V.; Electric Power Engineering, 1999.  
PowerTech Budapest 99. International Conference on, 29 Aug.-2 Sept. 1999.
- [5] The unified power flow controller: a new approach to power transmission control  
Gyugyi, L.; Schauder, C.D.; Williams, S.L.; Rietman, T.R.; Torgerson, D.R.; Edris, A.;  
Power Delivery, IEEE Transactions on, Volume: 10 Issue: 2, April 1995, Page(s): 1085 - 1097.

- 
- [6] Static Synchronous Series Compensator: A Solid-State Approach to the Series Compensation of Transmission Lines by Gyugyi, L.; Schauder, C.D.; Sen, K.K.; Power Engineering Review, IEEE, Volume: 17 Issue: 1, January 1997.
- [7] Dynamic compensation of AC transmission lines by solid-state synchronous voltage sources by Gyugyi, L.; Power Delivery, IEEE Transactions on, Volume: 9 Issue: 2, April 1994.
- [8] Gyugyi L, Sen K. K., Schauder C. D. "The Interline Power Flow Controller Concept: A New Approach to Power Flow Management in Transmission Systems" IEEE Transactions on Power Delivery. Vol 14 No 3, July 1999, pp 1115-1123.
- [9] Eckroad S., EPRI Technology review, "UPS substation TM, Control System Feasibility Evaluation", June 2000, pp 2-3, 2-9.
- [10] Mohaddes, M, Gole, A. M, McLaren P.G. "A neural network controlled Optimal Pulse-Width Modulated STATCOM". IEEE Transactions on Power Delivery, Vol 14 No 2, April 1999, pp 481-488.
- [11] Sen Kalyan K. "SSSC - Static Synchronous Series Compensator: Theory, Modeling and Applications". IEEE Transactions on Power Delivery, Vol 13 No 1, January 1998, pp 241-246.
- [12] Uzunovic Edvina, Cañizares Claudio A, Reeve John. 'Fundamental Frequency Model of Static Synchronous Compensator'. North American Power Symposium (NAPS), Laramie, Wyoming, October 1997, pp 49-54.

- 
- [13] Kumar S. L, Ghosh A. "Modeling and Control Design of a Static Synchronous Series Compensator". IEEE Transactions on Power Delivery, Vol 14 No 4, October 1999, pp 1448-1453.
- [14] Three phase load balancing STATCOM by Christopher Struthers M.Sc thesis (University of Manitoba-2002).
- [15] Grainger John J., Stevenson Jr. William D., Power System Analysis, 1994, McGraw Hill International Edition, Electrical Engineering Series, pp 342-344.
- [16] UPFC-unified power flow controller: theory, modeling, and applications, Sen, K.K.; Stacey, E.J.; Power Delivery, IEEE Transactions on, Volume: 13 Issue: 4, Oct. 1998 Page(s): 1453 -1460.
- [17] Power flow and transient stability models of FACTS controllers for voltage and angle stabilities studies, Claudio A Canizares , University of Waterloo.
- [18] Control design and simulation of Unified Power Flow Controller, K R Padiyar and A.M.Kulkarni , IIC Bangalore, India.
- [19] Control and Analysis of a Unified Power Flow Controller, Hideaki Fujita, Member, IEEE, Yasuhiro Watanabe, and Hirofumi Akagi, Fellow, IEEE.
- [20] Basic Control of Unified Power Flow Controller, I. Papic, IEEE transactions on Power Systems, vol 12, no4, Nov1997.
- [21] Mathematical analysis of FACTS devices based on a voltage source converter, I. Papic, eprj 56(200) 139-148.
- [22] C.schauder and H. Mehta, "Vector analysis and control of advanced static var compensators", IEEE fifth International Conference on AC and DC power Transmission, Sept 1991.
- .....

- 
- [23] IEEE Power System Fundamentals by Dr Bruce F. Wollenberg, Director of Graduate Studies at University of Minnesota (UM).
- [24] Power System Stability and Control, by Neal J. Balu, Mark G. Lauby (Editor) and Prabha Kundur .
- [25] Control of a unified power flow controller in fault recovery and with harmonic filter Mahanakom Univ. of Technol.; This paper appears in: Power Electronics and Variable Speed Drives, 2000. Eighth International Conference on (IEE Conf. Publ. No. 475).
- [26] Frequency response characteristics of the unified power flow controller Papic, I.; Gole, A.M.; Power Delivery, IEEE Transactions on, Volume: 18 Issue: 4, Oct. 2003 Page(s): 1394 -1402.